EXPERIMENTAL STUDY OF ENERGY DISTRIBUTION IN A TWO-DIMENSIONAL SUDDEN CONTRACTION

by

CHENG LUNG LIU

A THESIS

submitted to

OREGON STATE UNIVERSITY

in partial fulfillment of
the requirements for the
degree of

MASTER OF SCIENCE

June 1962

APPROVED:

[redacted]

Associate Professor of Department of Civil Engineering

In Charge of Major

[redacted]

Head of Department of Civil Engineering

[redacted]

Chairman of School Graduate Committee

[redacted]

Dean of Graduate School

Date thesis is presented May 17, 1962

Typed by Jolene Wuest

ACKNOWLEDGMENT

The author is very grateful to his major professor, Dr. Roy H. Shoemaker, for his advice and counseling through the period of this investigation. Special thanks are due to him for taking the photographs which are of significance in this experiment.

Sincere thanks are made by the author to other staff members of the Department of Civil Engineering and the Department of Electrical Engineering for providing part of the necessary apparatus and for their counseling for this investigation.

TABLE OF CONTENTS

Table of Contents (continued)

Table of Contents (continued)

Appendix

FIGURES

Figures (continued)

TABLES

NOTATION

A. Cross-sectional area of flow

B. Breadth of conduit

b. Distance between streamlines

D. Diameter of pipe

E. Euler number

E_L. Head loss

f. Frictional factor

g. Acceleration of gravity

H. Height of conduit

h. Piezometric head

K. Energy coefficient

K. Momentum coefficient

L. Length parameter

ℓ. Length of pipe

P. Pressure

Q. Rate of flow

R. Reynolds number

r. Hydraulic radius

V. Average velocity of flow

v. Local velocity

Z. Elevation head

Notations (continued)

γ. Specific weight of fluid

ρ. Mass density of fluid

ν. Kinematic viscosity of fluid

μ. Dynamic viscosity of fluid

S. Specific gravity of fluid

EXPERIMENTAL STUDY OF ENERGY DISTRIBUTION IN A TWO-DIMENSIONAL SUDDEN CONTRACTION

INTRODUCTION

One of the most important problems of pipe flow generally encountered in engineering practice is determination of head loss. For short pipes, the head loss caused by change of local boundary form often becomes more important than the head loss caused by boundary friction.

The head loss caused by any change of boundary geometry is the product of a loss coefficient and a velocity head. The loss coefficients for various boundary form changes have been determined experimentally for engineering practice.

Some work has been done on comparing the geometric as well as kinematic characteristics of submerged jet profile with that of free jet. (1, p. 1038-17). Heacock (3, p. 57) has found that the orifice contraction coefficients obtained by von Mises (6, p. 34) for two-dimensional fluid flow were valid for the three dimensional flow. No further finding has been reported on the comparison of free jet characteristics with the submerged confined jet which existed downstream of a pipe sudden contraction. No information appears to be available in the literature concerning the details of flow patterns as

well as energy dissipation across the flow transition zone, the region where streamlines converge and the velocity of flow increases.

Worth has found that about one-half of the head loss across a three dimensional pipe sudden contraction occurs upstream of the vena contracta (11, p. 40), a downstream section where the flow paths in jet are parallel. It was considered of interest to ascertain in what proportion energy will be dissipated in different portions of the transition zone of a two-dimensional sudden contraction.

Purposes

This experimental study was made to measure the energy distribution over the entire zone of flow acceleration of a two-dimensional pipe sudden contraction. Therefore, the rate of energy dissipation in this zone might be shown. Other purposes of this investigation were to study the characteristics of the two-dimensional confined jet existing downstream of the contraction and to investigate the effect of eddies around the jet periphery upon flow pattern.

The writer also intended to test the validity of the applicability of the assumption that the continuous flow domain in the acceleration zone of two-dimensional pipe sudden contraction may be treated as an irrotational flow pattern.

Scope

This experimental study was made under conditions in which a steady turbulent flow was maintained throughout a plexiglas conduit system. A sudden contraction was formed in the conduit in a manner such that no side contractions occurred. The ratio of the downstream conduit cross-sectional area to the upstream conduit cross-sectional area was equal to 1/2. The tests were conducted under room temperature.

THEORETICAL BACKGROUND

Turbulence Assumption

Flow in a confined conduit may be characterized by two dimensionless parameters, namely Reynolds number R and Euler number E.

Reynolds number R involves velocity V, length L, density ρ and viscosity μ. The form $R = VL\rho/\mu$ is obtained by dimensional analysis. This parameter may be considered to represent the ratio of the typical unit inertial force $\rho V^2/L$ to a typical unit viscous resistance $\mu V/L^2$. (6, p. 156). Therefore R shows the relative importance of viscous action in confined flow.

The length parameter L varies with boundary geometry. For pipe flow, the diameter of the pipe is considered as the length parameter. For flow in a rectangular conduit, four times the hydraulic radius, 4r replaces the L value for computation of equivalent Reynolds Number. The error introduced by this approximation will be negligible, however, so long as the height-width ratio of the conduit is not excessively great or small. (6, p. 216). Thus

$$R = 4Vr\rho / \mu = 4Vr / \nu \qquad (1)$$

It has been determined that in pipe flow at Reynolds numbers above 10^4 to 10^5 there is only a negligible degree of viscous effect on flow patterns (3, p. 25).

For the steady irrotational flow where only pressure difference, velocity and density are considered, the dimensionless ratio $\Delta p / \rho \frac{V^2}{2}$ will characterize the flow pattern. This ratio is known as the Euler number and may be written as

$$E = V / \sqrt{2\Delta p / \rho} \qquad (2)$$

Apparently, E will depend upon boundary geometry only when no other fluid property influences the flow (6, p. 62).

Therefore, for a certain boundary geometry, the Euler number will remain constant under the condition where the viscous effect on flow is negligible. This condition usually occurs when flow is at a high Reynolds number.

Two-dimensional Flow Assumption

For a two-dimensional steady irrotational flow, the fluid particle moves in only two directions in a plane, and same flow patterns exist in all parallel planes. No angular velocity of fluid particle exists in this flow pattern. With a steady rate of flow, the flow pattern will remain unchanged with time.

In a two-dimensional conduit, having a rectangular cross section with a relatively narrow width, flow may be considered two-dimensional, for the secondary flow in the direction normal to the side wall is eliminated by the close-spaced side walls. However, the existence of boundary shear along the side wall is expected to influence the flow pattern slightly. Therefore, flow patterns in central plane of a two-dimensional conduit will be subjected to a minimum influence by the boundary friction.

Because of the non-uniform distribution of velocities along the direction normal to the side walls of conduit, the average of measured central plane velocities will be higher than the true average velocity.

Correction factors are needed to reduce the measured velocities along central plane to their two-dimensional value. The variation of the factor is small across the cross section except at the zone near boundaries. The assumption of a constant correction factor for velocities in a two-dimensional conduit is thus made.

Flow Pattern

The flow patterns of a turbulent flow through a two-dimensional sudden contraction may be best studied by dividing the region into five parts as shown in Figure 1.

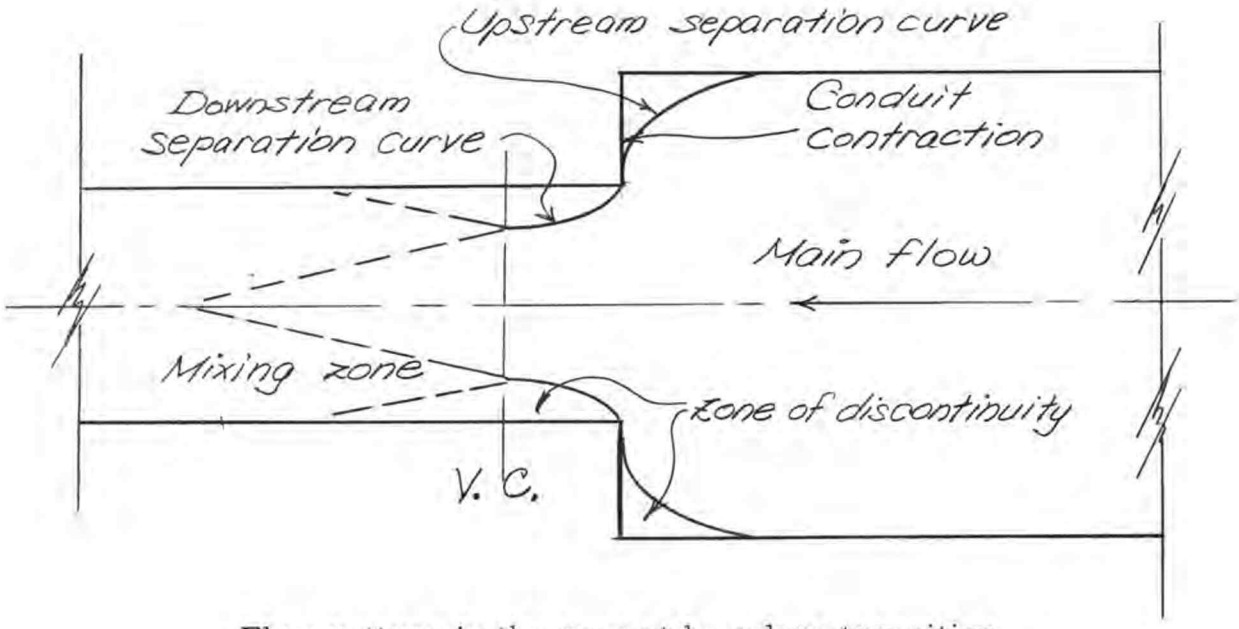

Flow pattern in the zone at boundary transition

Figure 1

The boundaries of conduit turn abruptly through two right angles to form the sudden contraction, and the upstream and the downstream separation curves were formed to separate the zones of discontinuity from the continuous main flow. The contracted flow domain may be considered as a confined jet, and the section V. C. where the jet reaches its minimum cross-section is called the vena contracta. (4, p. 120). Downstream from vena contracta, a large amount of eddy action exists in the zone where fluid carrying high kinetic energy is mixing with that of low kinetic energy near boundary.

Separation curve. As flow approaches the sudden contraction, the streamline along the upstream boundary must leave the boundary somewhere upstream from the contraction. Otherwise the streamline

would be required to turn abruptly through an angle of 90 degrees at the corner, which is physically impossible. A surface of discontinuity known as separation curve is thus formed between the main flow and the zone of discontinuity.

In like manner, the streamline is not able to follow the sharp-edged entrance to the downstream conduit and a downstream separation curve is thus formed. The upstream separation point at which the separation occurred is not clearly defined, but the downstream separation point is always located at the square-edged corner.

According to Dodge a layer of small eddies is generated along the surface of discontinuity downstream of the sudden contraction. This eddy layer is mainly caused by the discontinuity of velocity gradient across the separation curve. (2, p. 186-191). The formation of such a vortex blanket not only stimulates a turbulence over the downstream zone of separation but also starts a mixing zone as these eddies are carried downstream.

Upstream zone of discontinuity. Being confined by the conduit boundaries and surface of discontinuity, the zone of discontinuity upstream from contraction has a different flow pattern. The velocity gradient across surface of discontinuity causes turbulence in this zone.

The pressure intensity is essentially constant in the whole region. (8, p. 208). As the surrounding velocity is relatively lower than that in jet, the head loss due to eddy action in this zone is also relatively small.

Downstream zone of discontinuity. Unlike the upstream separation zone, the downstream zone of discontinuity has more complicated boundary conditions. Large unstable eddies exist between the surface of separation and conduit wall, causing fluctuation of the separation surface. No distinct downstream boundary of this eddy zone can be defined because of the great instability of surface of discontinuity downstream from vena contracta.

The energy dissipation into this zone is mostly caused by the turbulence in these large scale eddies and part of the head loss may be attributed to the vortex layer along separation curve. (2, p. 214, 8, p. 258).

Mixing zone. As the vortex blanket extends downstream beyond vena contracta and as the jet expands to fill the conduit, the effect of the deceleration of jet velocity and the existence of tangential stress around jet cause a thickening of the eddy blanket and form a mixing zone.

The turbulent mixing process causes an energy dissipation rate which is far greater than that occurring immediately upstream. (2, p, 213).

The effect of boundary contraction on the downstream flow pattern extends downstream until the flow attains the normal velocity distribution in the smaller conduit.

Main flow. The continuous flow domain bounded by conduit walls and separation curves may be defined as the main flow region; in this region the condition of flow continuity is fulfilled.

According to Prandtl's boundary layer theory, for fluid with relatively small viscosity, the internal friction is not appreciable except in a thin layer along boundary of fluid. Therefore, as long as the boundaries remain straight the turbulent flow domain outside the thin layer along boundary may be assumed to be ideal flow, that is, frictionless flow. Rouse (6, p. 23, 233) has stated that so long as boundary form is such that the stream lines converge, the velocity distribution across the normal line becomes more uniform and the flow is thus more like an irrotational flow pattern. In a boundary condition of a sudden contraction, if the form of the separation can be determined, an irrotational flow may still be assumed for the flow domain upstream from vena contracta.

Flow Net

A flow net concept is used to help solve irrotational flow problems. If points of equal velocity potential are connected by a line, this line may be defined as an equipotential line. It has been

shown that equipotential lines are the orthogonal trajectories of the stream lines and thus intersect the stream lines at right angles. (9, p. 245). A flow net is thus composed of a family of equipotential lines and a family of streamlines in such manner that the configuration of the net is formed by many square grids.

The flow net can be constructed graphically by eye. Because of the similarity between the velocity potential field and the electric potential field, an electrical analogue device may be employed to determine the equipotential lines with the boundary condition known.

In order to fulfill the flow continuity, the velocity at different sections of flow path must be inversely proportional to the ratio of the breadths of path at the respective sections. Thus

$$\frac{V_1}{V_2} = \frac{b_2}{b_1} \qquad (1)$$

Therefore the distribution of velocity in terms of approaching velocity may be obtained simply by measuring the normal distances between adjacent streamlines.

Head Loss

Head loss in transition zone. If an assumption of irrotational flow is made for the transition zone of a sudden contraction, the Bernoulli theorem may be applied to points either along a streamline or along a normal line. (6, p. 49).

Bernoulli's theorem may be derived by integrating the Euler equation along a streamline. (6, p. 80). It states

$$\frac{v_1^2}{2g} + \frac{P_1}{\gamma} + z_1 = \frac{v_2^2}{2g} + \frac{P_2}{\gamma} + z_2 \qquad (4)$$

In which v_1, v_2 denote the upstream and downstream velocities, P_1, P_2 the pressures, and z_1, z_2 the respective elevations.

In real flow, Eq.(4) may be written along a streamline adding a head loss term E_L.

$$\frac{v_1^2}{2g} + \frac{P_1}{r} + z_1 = \frac{v_2^2}{2g} + \frac{P_2}{r} + z_2 + E_L \qquad (5)$$

where E_L is the head loss caused by viscous action between points 1 and 2. If each side of Eq.(5) is modified by downstream velocity head $v_2^2/2g$, after rearranging terms head loss may be expressed in terms of $v_2^2/2g$

$$\frac{\frac{E_L}{v_2^2}}{2g} = \frac{\frac{\Delta h}{v_2^2}}{2g} - \left[1 - \left(\frac{v_1}{v_2}\right)^2\right] \qquad (6)$$

where $\Delta h = \frac{P_1}{\gamma} + z_1 - \frac{P_2}{\gamma} - z_2$ is piezometric head difference.

Head loss between two sections. The total head loss between two sections of a confined conduit may be calculated by either energy theorem or the combination of Bernoulli's theorem and momentum principle.

The former may be derived from Newton's law and is expressed

$$(P_1 + \gamma Z_1 - P_2 - \gamma Z_2) Q = Ke_2 Q \frac{\rho V_2^2}{2} - Ke_1 Q \frac{\rho V_1^2}{2} \quad (7)$$

where $Ke = \frac{1}{A}\int \left(\frac{v}{V}\right)^3 dA$ (8)

is known as energy coefficient. (6, p. 112).

For two-dimensional conduit with constant breadth B,

$$K_e = \frac{1}{H}\int \left(\frac{v}{V}\right)^3 dH \quad (9)$$

where H = A/B.

Thus the energy loss between two sections may be calculated if the average velocities, energy coefficients and the pressures at both sections are known.

$$E_L = \Delta h - \left[Ke_2 \frac{V_2^2}{2g} - Ke_1 \frac{V_1^2}{2g}\right] \quad (10)$$

The energy equation can not be used under conditions where pressure across the section is not uniform. A combination of the Bernoulli theorem and the momentum principle yields an equation containing no pressure term. (10, p. 180).

The momentum equation for one-dimensional flow may be expressed

$$\Sigma F = K_{m2} Q \rho V_2 - K_{m1} Q \rho V_1 \quad (11)$$

in which $K_m = \frac{1}{H}\int \left(\frac{v}{V}\right)^2 dH$ (12)

is defined as the coefficient of momentum for two-dimensional conduit.

If shear stresses along boundaries are assumed negligible, the left side of Eq. (11) should be

$$\Sigma F = P_1 A_2 - P_2 A_2 \tag{13}$$

By combining Equation (11) and Equation (13) and rearranging terms

$$\Delta h = (P_1 - P_2)/\gamma = V_2(K_{m2}V_2 - K_{m1}V_1)/g \tag{14}$$

Substituting Equation (14) into Equation (10), and rearranging terms, the head loss E_L may be expressed

$$E_L = \left[(2K_{m2} - K_{e2})V_2^2 - 2K_{m1}V_1V_2 + Ke_1V_1^2\right]/2g \tag{15}$$

Head loss due to friction In pipe flow, the head loss due to turbulent flow may be calculated by the form

$$E_L = f\frac{\ell}{D}\frac{V^2}{2g} \tag{16}$$

For uniform flow assuming friction factor f constant, the head loss E is proportional to length of pipe.

$$E_L = K\ell \tag{17}$$

where K is a coefficient determined by experiment. If pipe diameter D in Equation (12) is replaced by 4r for rectangular conduit, Equation (13) will still be valid.

EXPERIMENTAL APPARATUS

Water Channel Projector

As a preliminary test, an observation of approximate flow pattern was made by means of a water channel projector. The apparatus was made by Ann Arbor Instrument Works, consisting of a water table and a specially devised projector as shown schematically in Figure 2.

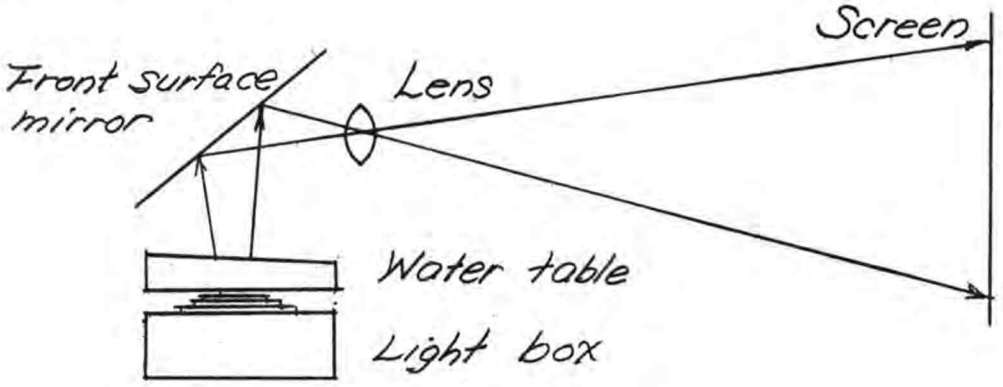

Figure 2 Water Channel Projector

Water flow was circulated in the water channel, which formed part of the water table, by a small pump. A solid block was placed in the channel to form the bottom half of the sudden contraction boundary, and flow pattern was displayed by shadows created by lycopium powder sprinkled on the surface of the water.

Main Model

The main test section was a transparent plastic rectangular conduit, 0.2 foot wide, 1 foot high and 7 1/2 feet long, to which was attached immediately downstream a smaller conduit of same width, 1/2 foot high and 4 feet long, as shown in Figure 3 and Figure 4. The two-dimensional sudden contraction was formed at the juncture of the conduits as may be seen from Figure 5.

The side walls of conduits were built of 1/4 inch plexiglas and the top and bottom of the conduits were constructed using 3/8 inch material. One and one-half inches wide reinforcing strips of 3/8 inch plexiglas were placed every 2 feet outside the large conduit.

One of the side walls of boundary transition zone was made removable so that piezometric holes along the separation curves could be drilled accurately after separation curves had been determined.

Water Flow System

Figure 7 shows schematically the arrangement of the water system used for this experiment. The rate of flow was controlled by the 4 inch valve located at the conduit upstream of the test section in order to assure homogeneous turbulent flow.

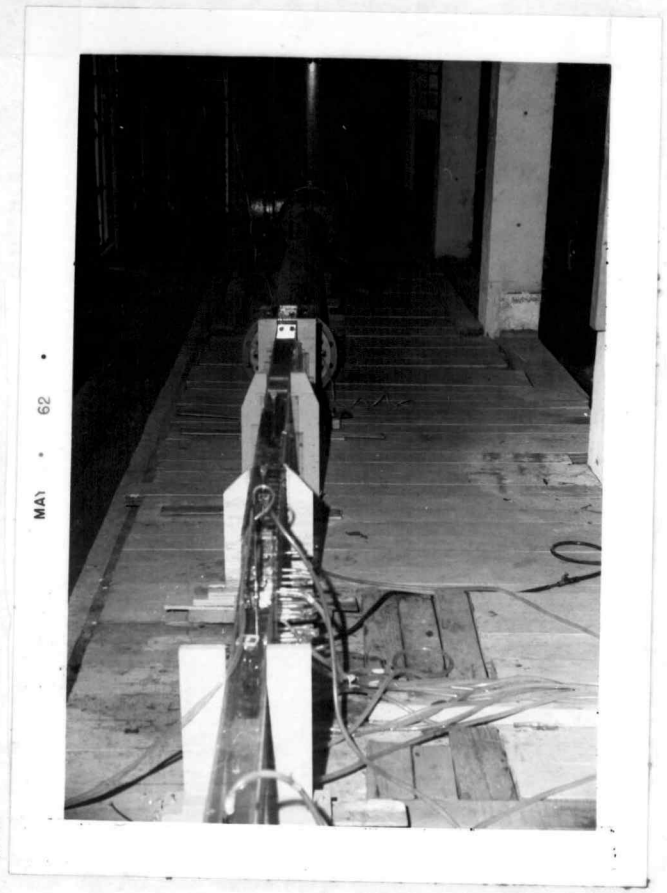

Stilling tank and testing system

Figure 3

Testing section and outlet of conduit

Figure 4

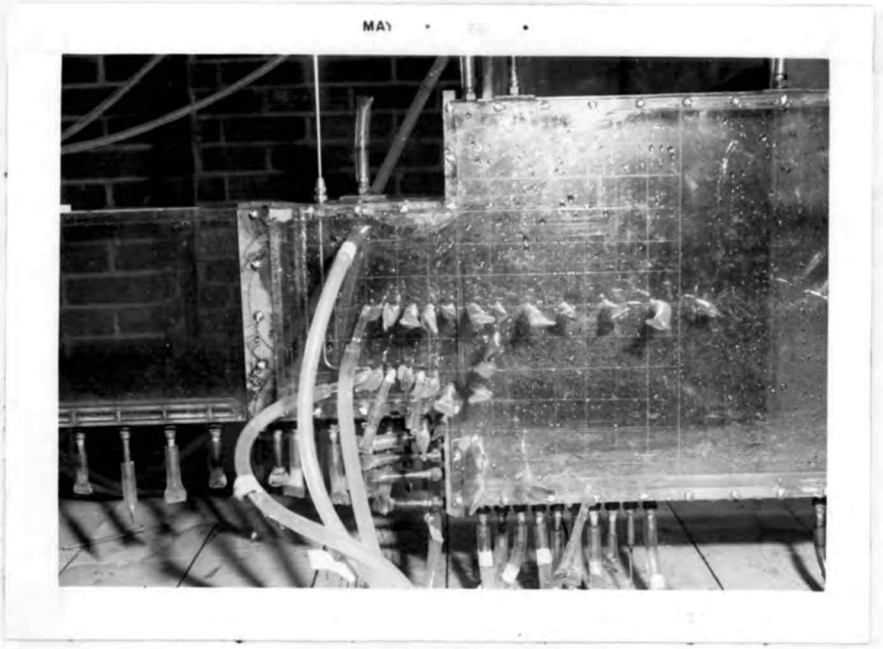

Removable side wall of model

Figure 5

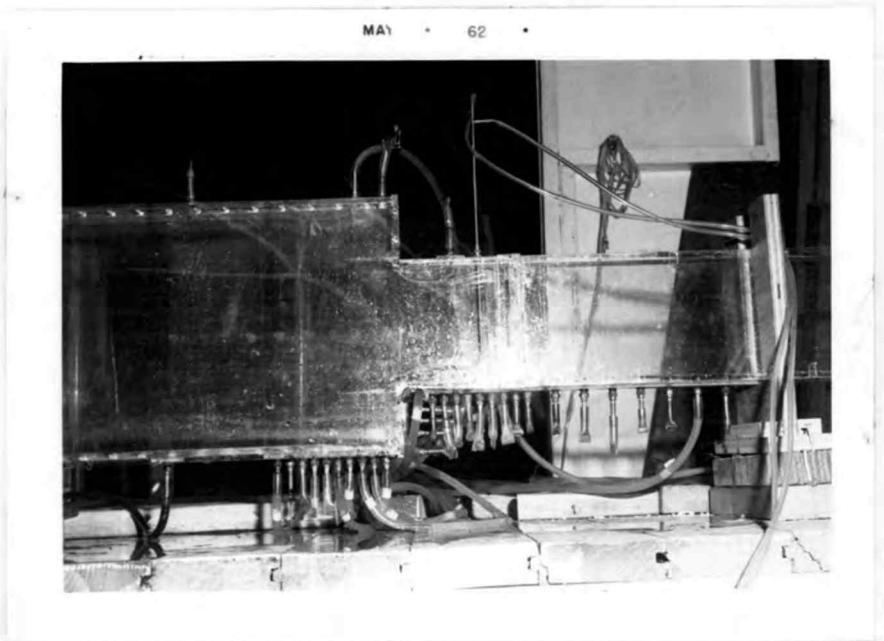

Locations at piezometric pressure taps along boundary and pilot tube in use

Figure 6

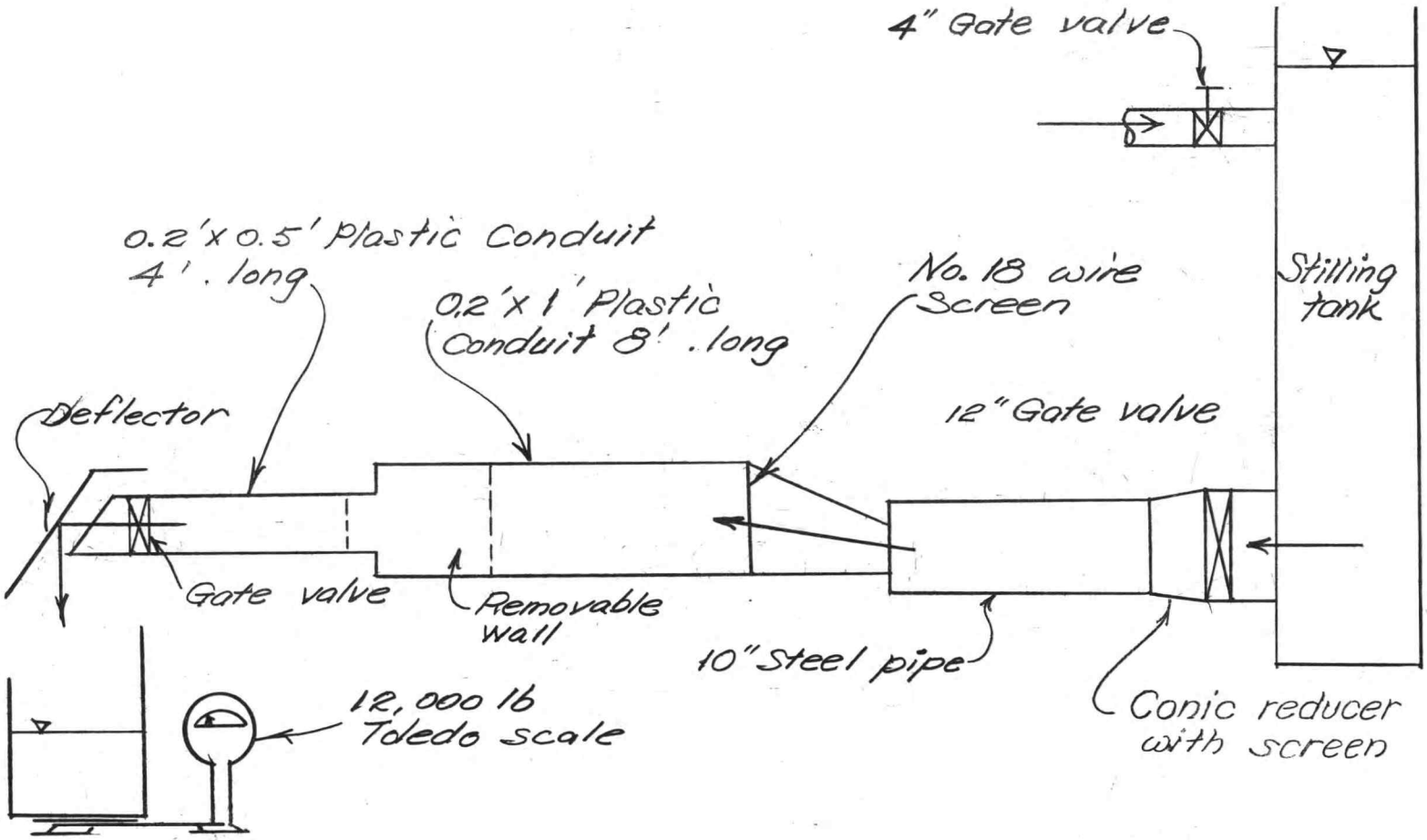

Apparatus arrangement

Figure 7

Piezometric Head Measurement

In order to measure piezometric head either along the bottom of the conduit or along the separation curves, holes were drilled by a 1/16 inch drill through the wall, and were beveled slightly on the inside of the wall with larger drill to insure no burrs.

Two types of piezometric connections were used and are shown in Figure 8. Type A connections were installed at the bottom of the conduit while type B connection were employed on the removable side wall. One-fourth inch I. D. Tygon tubing was used to connect the pressure taps to the piezometer columns. When a pressure tap was not in use, it was sealed with a short section of Tygon tubing which had been fused at one end, as shown in Figure 5. The location of pressure taps along the bottom of the conduit is presented in Table 1 and is shown in Figure 6 and Figure 10.

The piezometer board consisted of fifteen rigid transparent plastic tubes of 1/2 inch I. D.. Movable boards with graduations of 0. 01 foot were positioned on the main board enabling a reading to the nearest 0. 005 foot. The board was constructed by Worth for his master's thesis experiment.(11, p.15). Figure 9 shows the main part of piezometric board. Two smaller tubes at the right were not used in this test.

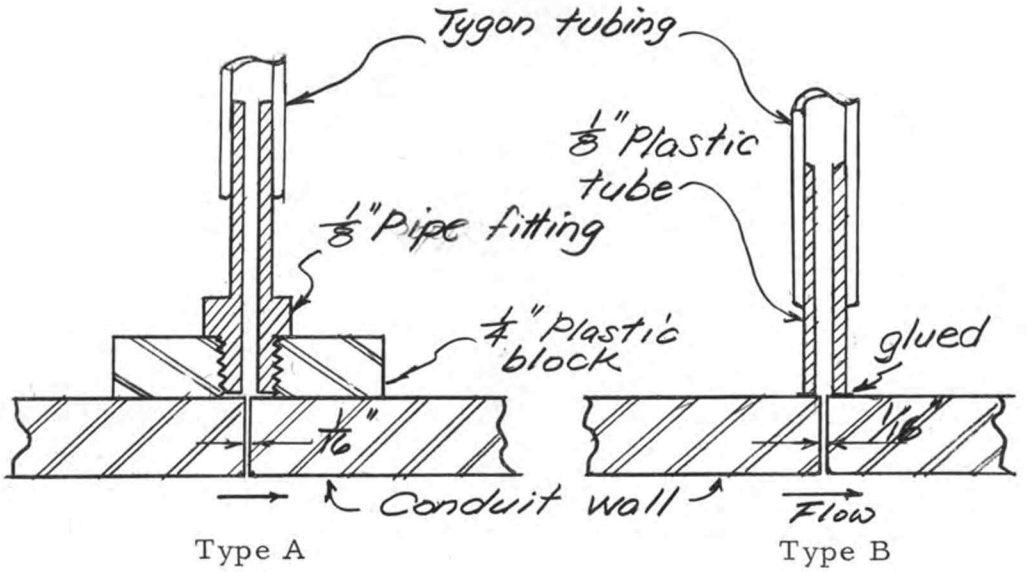

Pressure tap connections

Figure 8

Piezometer board

Figure 9

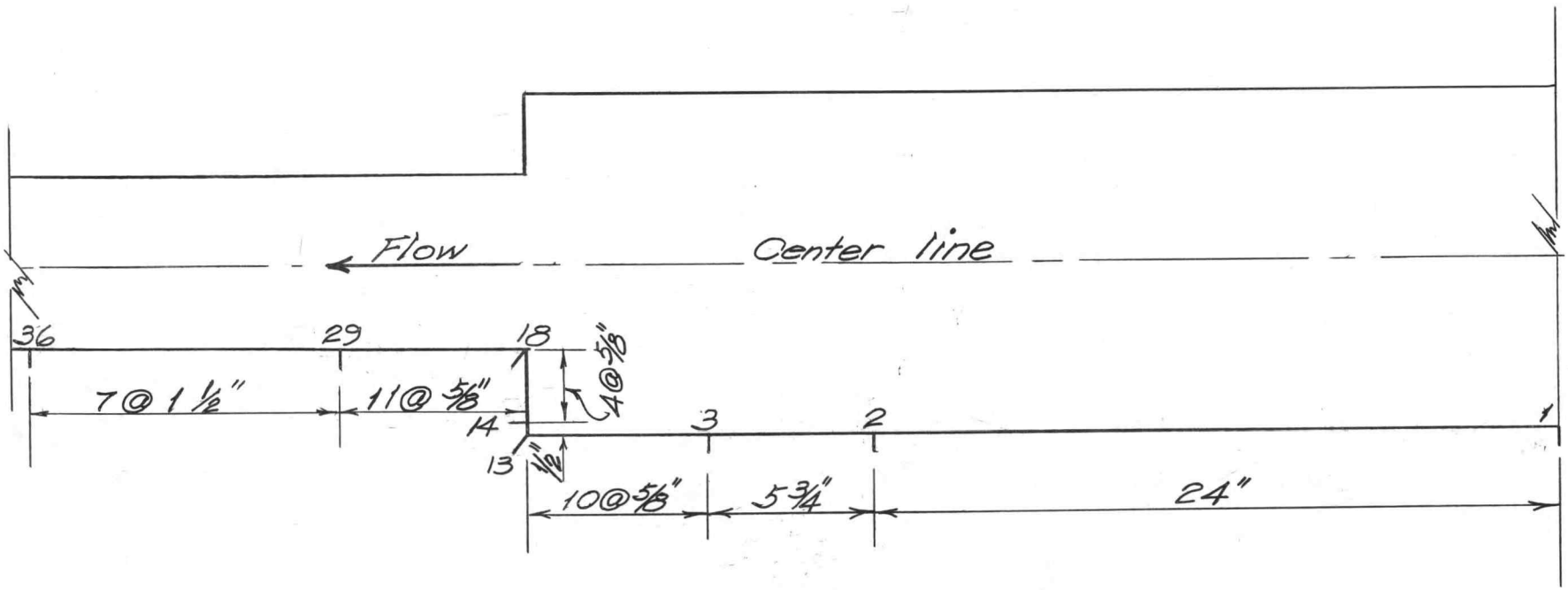

Location of pressure taps along boundaries

Figure 10

Table 1

Locations of piezometric head connections along boundaries

Tap No.	Distance from contraction	Tap No.	Distance from contraction
1	3 ft.	22	- 2 1/2 inches
2	1 ft.	23	- 3 1/8 inches
3	6 1/4 inches	24	- 3 3/4 inches
4	5 5/8 inches	25	- 4 3/8 inches
5	5 inches	26	- 5 inches
6	4 3/8 inches	27	- 5 5/8 inches
7	3 3/4 inches	28	- 6 1/4 inches
8	3 1/8 inches	29	- 6 7/8 inches
9	2 1/2 inches	30	- 8 3/8 inches
10	1 7/8 inches	31	- 9 7/8 inches
11	1 1/4 inches	32	- 11 3/8 inches
12	5/8 inch	33	- 12 7/8 inches
13	0 inches	34	- 14 3/8 inches
19	- 5/8 inch	35	- 15 7/8 inches
20	- 1 1/4 inches	36	- 17 3/8 inches
21	- 1 7/8 inches	100	- 3 feet

(+) sign = upstream
(-) sign = downstream

Velocity Measurement

Holes of 3/8 inch diameter were drilled at the top of the pipe at the locations 10.5 inches upstream, 4.5 inches downstream and 3 feet downstream from sudden contraction. These holes were tapped inside to fit the pitot tube.

A 1/8 inch diameter Prandtl type pitot tube having 1 1/2 inch tip was employed to measure the velocity of flow. The tube was arranged so that it could slide in a 1/8 inch copper pipe fitting and could be fixed by chuck on the top of the fitting. Figure 5 and Figure 6 show the pitot tube in use. The stagnation pressure end and the static pressure end were connected to each end of a manometer.

In order to increase the sensitivity of the manometer reading, dyed chloroform was placed in the bottom half of the U tube. The specific gravity of chloroform was found to be 1.47 for which calculations are shown in the appendix.

Separation Curve Determination

Either dye or air bubbles were injected into the flow to determine the separation curves.

The instrument used for dye injection into conduit consisted of 1/8 inch I.D. Tygon tubing. Two small valves were installed in this

system to control the outflow of dye, which was a concentrated solution of potassium permanganate.

Air bubbles were injected into the main flow by a bicycle hand pump for the purpose of determining separation curves. The outlet tubing was led into the conduit at the end of 10 inch steel pipe and a perforated glass filter was attached at the end.

Electrical Apparatus

Equipotential lines were obtained by means of an electrical apparatus (5, p. 62), which is shown in Figure 11. In order to obtain a higher sensitivity of earphone perception, an oscillator is employed to produce a 1000-cycle audio signal. On the bottom of the tray rectangular ordinates were marked so that detected points could be easily plotted on graph paper.

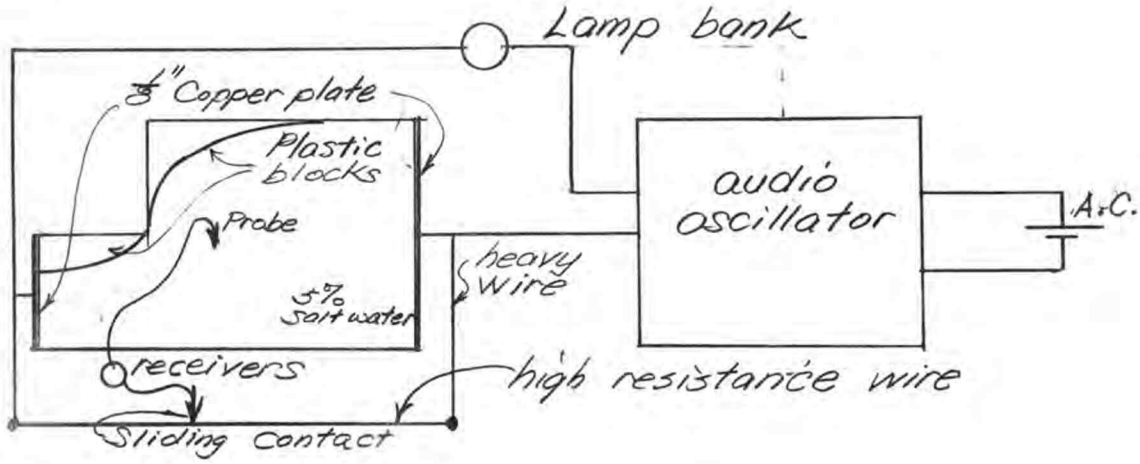

Electrical aparatus

Figure 11

EXPERIMENTAL PROCEDURES

Flow Pattern Observation

Before constructing the testing model, the approximate flow pattern which would exist in the transition zone of the sudden contraction was first inspected by the water channel projector. The plastic block was so placed in the uniform water channel that a boundary form was produced similar to half that of the prototype (assuming the flow pattern was symmetrical about the centerline of the conduits).

After the model was constructed and installed, the flow pattern was then inspected by the help of dye injection. Dye was injected through different pressure connections along the boundary.

Rate of Flow Determination

In order to eliminate viscous influence on flow pattern, a high Reynolds number flow is required for this test.

A stable head was first maintained in the stilling tank by adjusting the 4 inch control valve. The rate of flow as well as the piezometric pressure difference between upstream pressure connection No. 1 and downstream pressure connection No. 36 were

measured concurrently. The control valve was then readjusted allowing different discharges and other sets of data were obtained. Six readings were made in the first test and three more were measured to provide better data for the plotting of Euler versus Reynolds number curve.

Measured pressure differences and calculations of rate of flow are presented in Table 2. From these data, Euler numbers and Reynolds numbers were computed as shown in Table 3. The curve is shown in Figure 12. The rate of flow 0.321 cubic feet per second was chosen from the plotted curve and was used throughout the main experiment.

Determination of Separation Curve

After the flow of chosen discharge was established in the model, air bubbles were injected into the approaching flow. Photographs were taken at the time a group of air bubbles had just reached the separation regions. Pictures of downstream separation zone with dye injecting through pressure tap No. 18 at the sharp-edged corner were also taken. A total of 20 separate photographs were taken in order to obtain the average separation curves using method of superposition.

Table 2

Rate of flow and corresponding pressure differences

		1	2	3	4	5	6	7	8	9
W lb.		500	500	1000	1000	1000	1000	1000	500	200
time, sec.	1	34.	20.	33.0	30.0	27.3	24.6	22.1	38.4	37.3
	2	34.5	19.5	32.5	30.0	26.6	25.8	22.5	38.6	38.0
	3	34.5	20	31.9	30.0	27.3	24.2	22.1	39.2	34.8
	4	35	19	32.6	30.0	25.8	25.2	22.2	39.4	34.7
	5	34	19.5			26.4	25.7	22.5		
	6	33.8	20			27.4				
	7		19.5			26.8				
Σ		206.2	137.5	130	120	187.6	125.5	111.4	155.6	144.8
Average		34.4	19.65	32.5	30	26.8	25.1	22.3	38.9	36.2
Q		0.233	0.408	0.492	0.534	0.598	0.639	0.719	0.206	0.089
P*		0.086	0.233	0.366	0.459	0.584	0.652	0.756	0.082	0.014

* Piezometric head differences were measured between pressure tap (1) and pressure tap (36).

Table 3

Computations for Euler and Reynolds numbers

1	2	3	4	5	6	7
No.	Q	(2) x C_1 V	Δh	(4) $\sqrt{\Delta h}$	(3)x$C_2/10^4$ R $/10^4$	$\frac{(3)}{(5)}$ X C_3 E
	c. f. s.	ft. /sec.	ft.	ft.		
1	0.089 *	0.89	0.014	0.118	2.07	0.940
2	0.206 *	2.06	0.082	0.286	4.79	0.898
3	0.233 **	2.33	0.086	0.293	5.5	0.991
4	0.408 **	4.08	0.233	0.483	9.62	1.050
5	0.492 **	4.92	0.366	0.605	11.46	1.011
6	0.534 **	5.34	0.459	0.678	12.43	0.979
7	0.598 **	5.98	0.584	0.765	13.94	0.975
8	0.639 **	6.39	0.652	0.808	14.90	0.984
9	0.719 *	7.19	0.756	0.870	16.75	1.029

$C_1 = \frac{1}{A} = 10$

$C_2 = \frac{4r}{\nu} = \frac{4(0.0714)}{1.21(10)^{-5}} = 2.36\ (10)^4$

$C_3 = \frac{1}{\sqrt{2g}} = 0.1245$

* Temperature 16.8° C.

** Temperature 15.8° C.

Computations for Euler and Reynolds numbers

Table 3

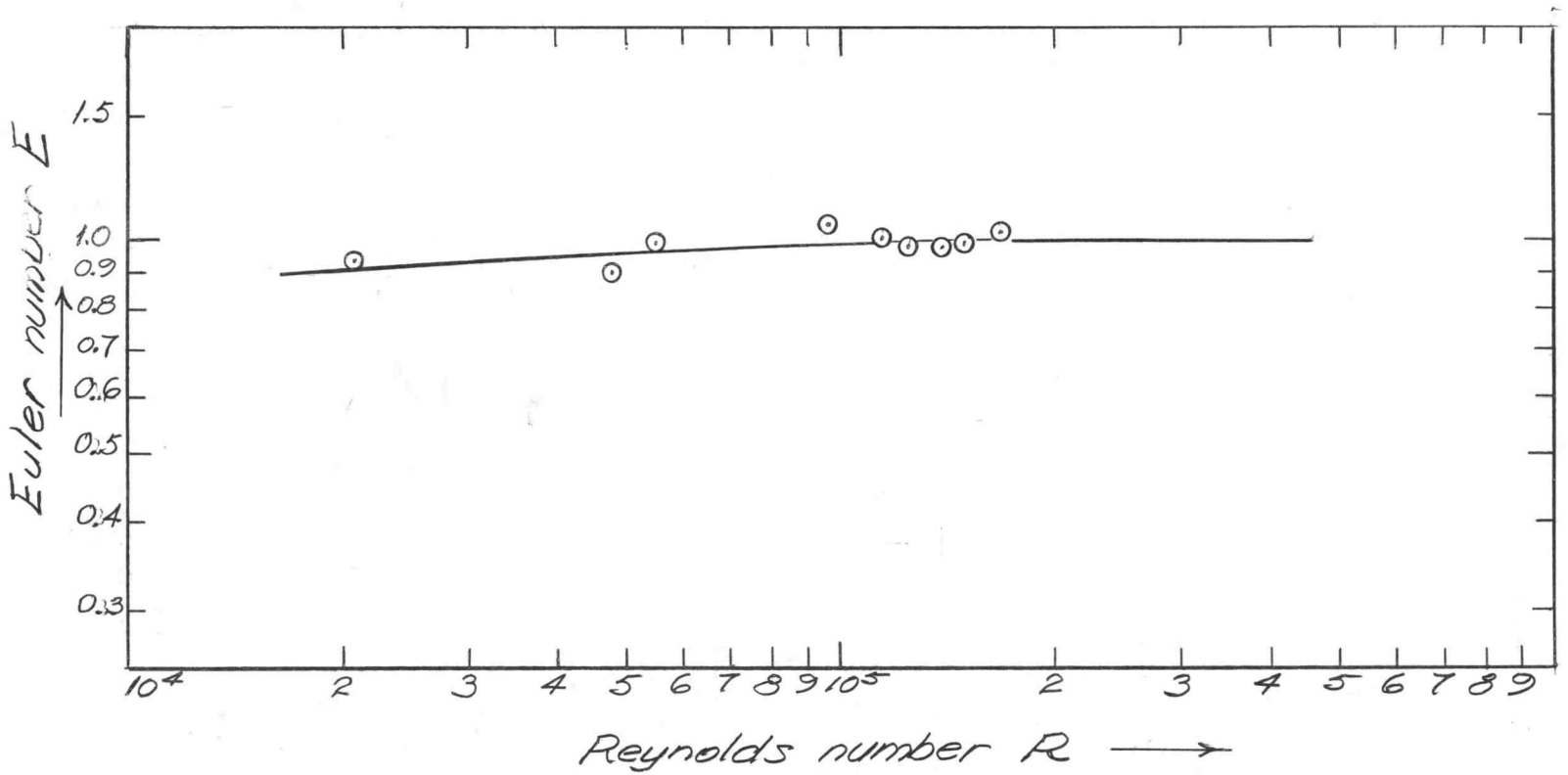

Euler versus Reynolds number curve

Figure 12

Construction of Flow Net

The electrolyte tray used in electrical apparatus was then constructed using the determined separation curves as part of boundaries, as shown in Figure 11. To determine equipotential lines, the probe pencil was moved in tray until the hum in the earphone stopped. The point under the probe was plotted on the graph paper. Several such points were determined and formed an equipotential line. Other such lines were found by moving the sliding contact to new stations.

The flow net was constructed by eye with the help of determined equipotential lines, and was carefully checked by diagonals.

In order to measure pressure along the surfaces of discontinuity, separation curves were marked on the removable wall piece and type B pressure connections were installed at every net joint along separation curves and center line.

Piezometric Pressure and Velocity Traverse

The head water was observed to rise with time, and the rate of flow was difficult to stabilize. It was found that the upstream No. 18 wire screen had been collecting rusting material with a resultant

increase in head loss across the screen. This increasing head loss reduced the rate of flow and thus caused the rising of the head water level.

Rate of flow was measured every half hour or less, and a curve of discharge versus time was thus plotted. For every measurement of velocity, time was also recorded. Approximately two hours were needed to take a velocity traverse. Piezometric pressures were measured by groups, each time 15 pressure readings were taken concurrently. From each group, two pressure taps were chosen to form a new group and piezometric pressures were then measured under desired discharge, 0.321 cubic feet per second.

All the measured values had been carefully examined, and any unreasonable data were rechecked.

After the main test had been accomplished, dye was used for final flow pattern observation trying to find more information about the characteristics of separation zones.

EXPERIMENTAL RESULTS

Figure 13 and Figure 14 are representative photographs taken for the purpose of determining separation curves. The average separation curves are presented in Figure 15 showing the superposed data.

The measured piezometric pressure data as well as computations for pressure correction are listed in Tables 4, 5, 6, 7, 8 and 9. The dimensionless plots for piezometric pressure differences are presented in Figures 16, 17, 18, 19, 20, 21, 22, 23 and 24. Measured pressure across section 3 inches downstream from contraction is plotted in Figure 30 in the appendix.

The results of velocity measurements and the calculations of velocity corrections for three different cross-sections are presented in Tables 10, 11 and 12. The discharge-time curve is plotted in Figure 25. The corresponding velocity profiles are plotted Figures 26, 27 and 28. The computations of energy coefficients and momentum coefficients are presented in Tables 13, 14 and 15 in appendix.

The measured equipotential lines by electrical apparatus and the flow net configuration in true scale are shown in Figure 29, in which the locations of the pressure connections along separation curves as well as along center line of conduit are also numbered.

The calculations of head losses using Equation 10 and Equation 15 are presented in appendix.

Results of flow pattern observation will be presented and discussed in the next section.

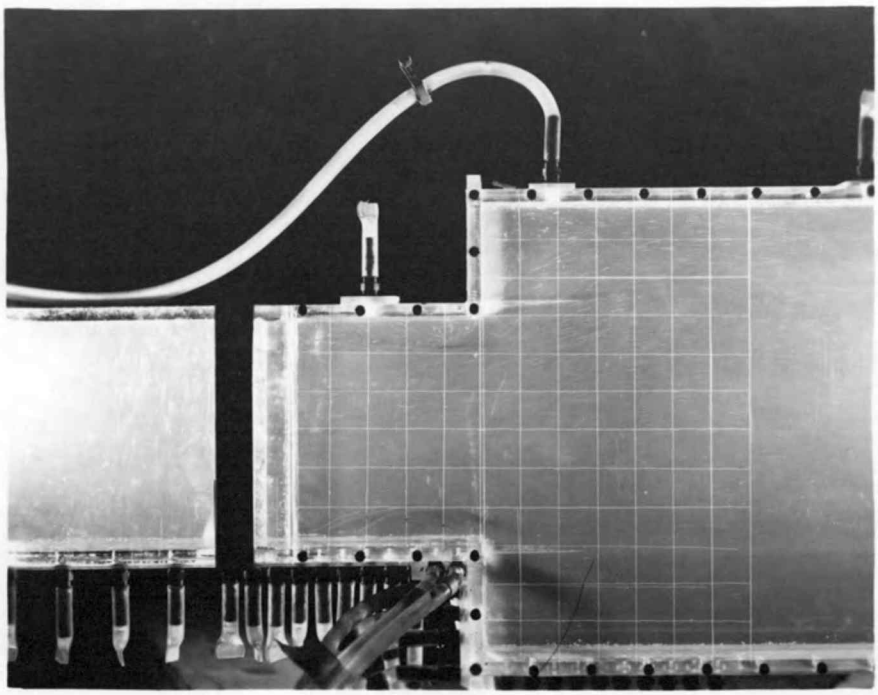

Figure 14

Flow pattern in flow transition zone shown by injected air bubbles

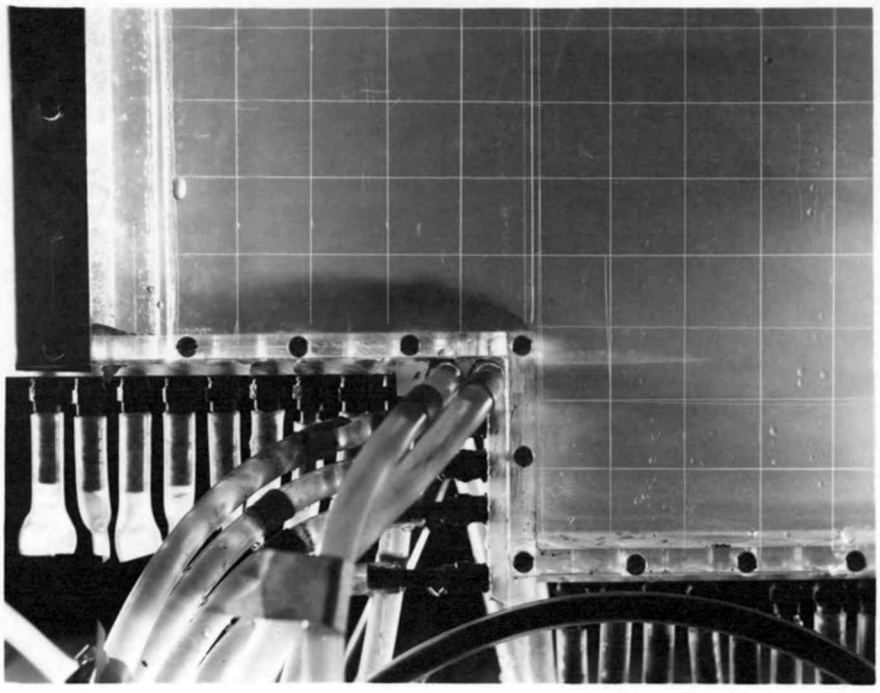

Figure 13

Downstream zone of separation indicated by dyed water

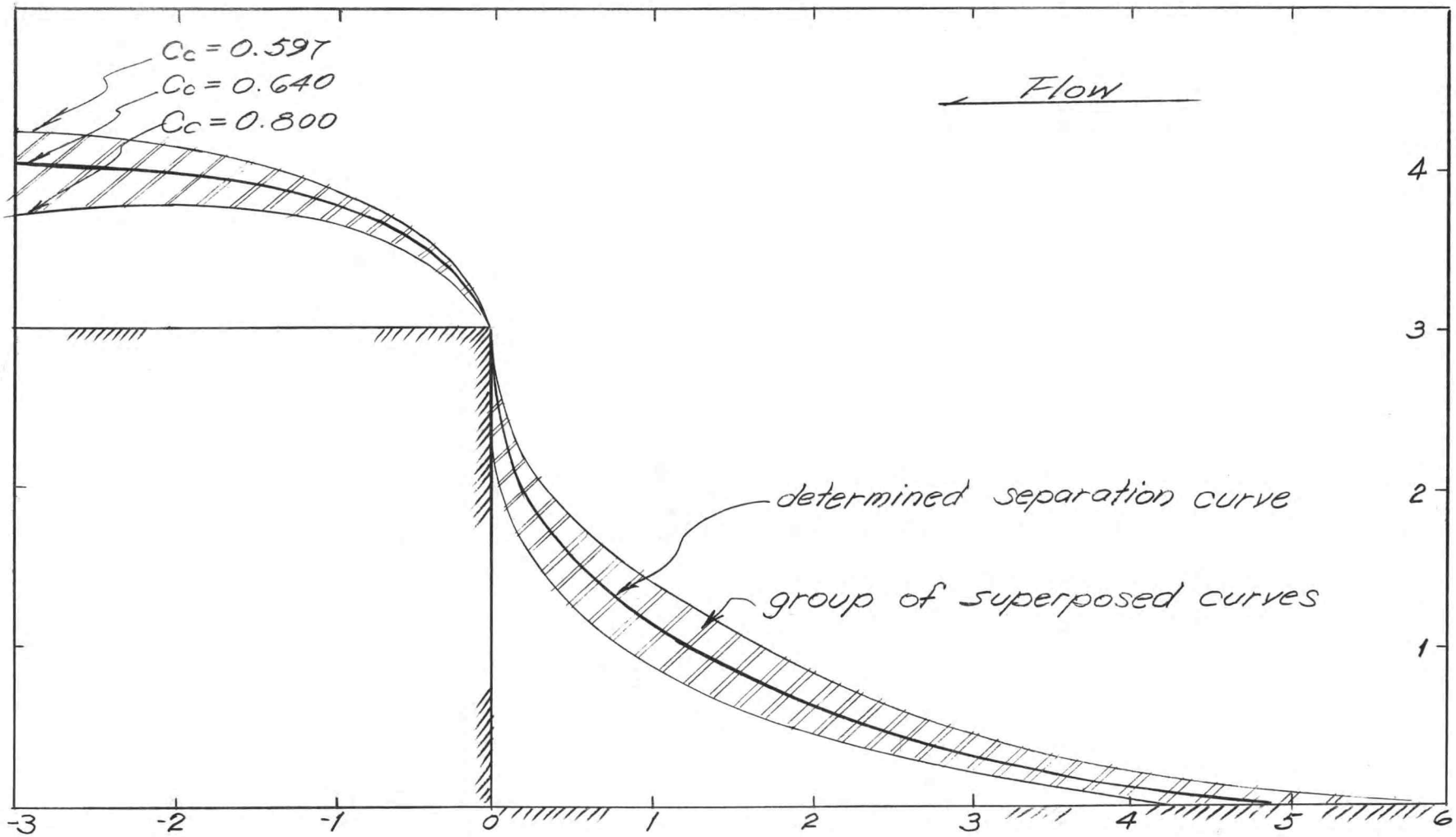

Figure 15. Average separation curves determined by method of superposition

Table 4

Head along upstream boundary

Tap Number	Measured Head h feet
1	0.929
2	0.920
3	0.925
4	0.928
5	0.930
6	0.931
7	0.932
8	0.932
9	0.929
10	0.929
11	0.929
12	0.929
13	0.929

Table 5

Head along vertical boundary

Tap Number	Measured Head h feet
13	0.929
14	0.929
15	0.934
16	0.935
17	0.926
18	0.679

Table 6

Head along downstream boundary

Tap Number	Measured Head h (ft)	Head difference Δh (ft)	Corrected difference Δhc (ft)	Corrected Head hc (ft)
19	0.482	0.078	0.154	0.558
20	0.480	0.080	0.158	0.554
21	0.485	0.075	0.148	0.564
22	0.493	0.067	0.132	0.580
23	0.510	0.050	0.099	0.613
24	0.530	0.030	0.059	0.653
25	0.547	0.013	0.026	0.686
26	0.550	0.010	0.020	0.692
27	0.556	0.004	0.008	0.704
28	0.558	0.002	0.004	0.708
29	0.560	0.000	0.000	0.712
	$\frac{0.712 - 0.558}{0.560 - 0.482} = \frac{0.154}{0.078} = 1.975$			
29	0.646	0.017	0.010	0.712
30	0.640	0.011	0.007	0.709
31	0.641	0.012	0.007	0.709
32	0.639	0.010	0.006	0.708
33	0.638	0.009	0.005	0.707
34	0.633	0.004	0.002	0.704
35	0.630	0.001	0.001	0.703
36	0.629	0.000	0.000	0.702
	$\frac{0.712 - 0.702}{0.646 - 0.629} = \frac{0.010}{0.017} = 0.588$			

piezometric head at section 3 feet ownstream from contraction = 0.682 (No. 100)

Table 7

Head along center line of flow transition zone

Tap No.	Measured Head h feet	Head difference Δ h feet	Checking Head hc feet	Corrected difference Δhc feet	Corrected Head hc feet
37	0.800	0.203	0.900	0.224	0.904
38	0.794	0.197		0.217	0.897
39	0.790	0.193		0.212	0.892
40	0.780	0.183		0.202	0.882
41	0.764	0.167		0.184	0.864
42	0.739	0.142	0.832	0.156	0.836
43	0.708	0.111		0.122	0.802
44	0.675	0.078		0.086	0.766
45	0.642	0.045		0.050	0.730
46	0.620	0.023		0.025	0.705
47	0.607	0.010		0.011	0.691
48	0.600	0.003		0.003	0.683
49	0.597	0.000	0.680	0.000	0.680

$$\frac{0.068}{0.061} = 1.115$$

$$\frac{0.220}{0.203} = 1.085$$

$$\frac{1.115 + 1.085}{2} = 1.1$$

Table 8

Head along separation surfaces

Tap Number	Measured Head h	Head difference Δh	Corrected difference Δhc	Corrected Head hc
50	0.816	0.260	0.306	0.910
51	0.816	0.260	0.306	0.910
52	0.816	0.260	0.306	0.910
18	0.620	0.064	0.075	0.679
53	0.560	0.004	0.005	0.609
54	0.553	- 0.003	- 0.004	0.600
55	0.547	- 0.009	- 0.011	0.593
56	0.544	- 0.012	- 0.014	0.590
57	0.545	- 0.011	- 0.013	0.591
58	0.552	- 0.004	- 0.005	0.599
59	0.556	0.000	0.000	0.604

$$\frac{0.306}{0.260} = 1.18$$

Table 9

Head along a normal line

Tap Number	Measured Head h' (ft)	Head difference $\Delta h'$ (ft)	Corrected difference Δhc (ft)	Corrected Head hc (ft)
42	0.729	0.097	0.153	0.832
62	0.728	0.096	0.152	0.831
61	0.722	0.090	0.142	0.821
60	0.703	0.071	0.112	0.791
18	0.632	0.000	0.000	0.679

$$\frac{0.832 - 0.791}{0.729 - 0.703} = \frac{0.041}{0.026} = 1.58$$

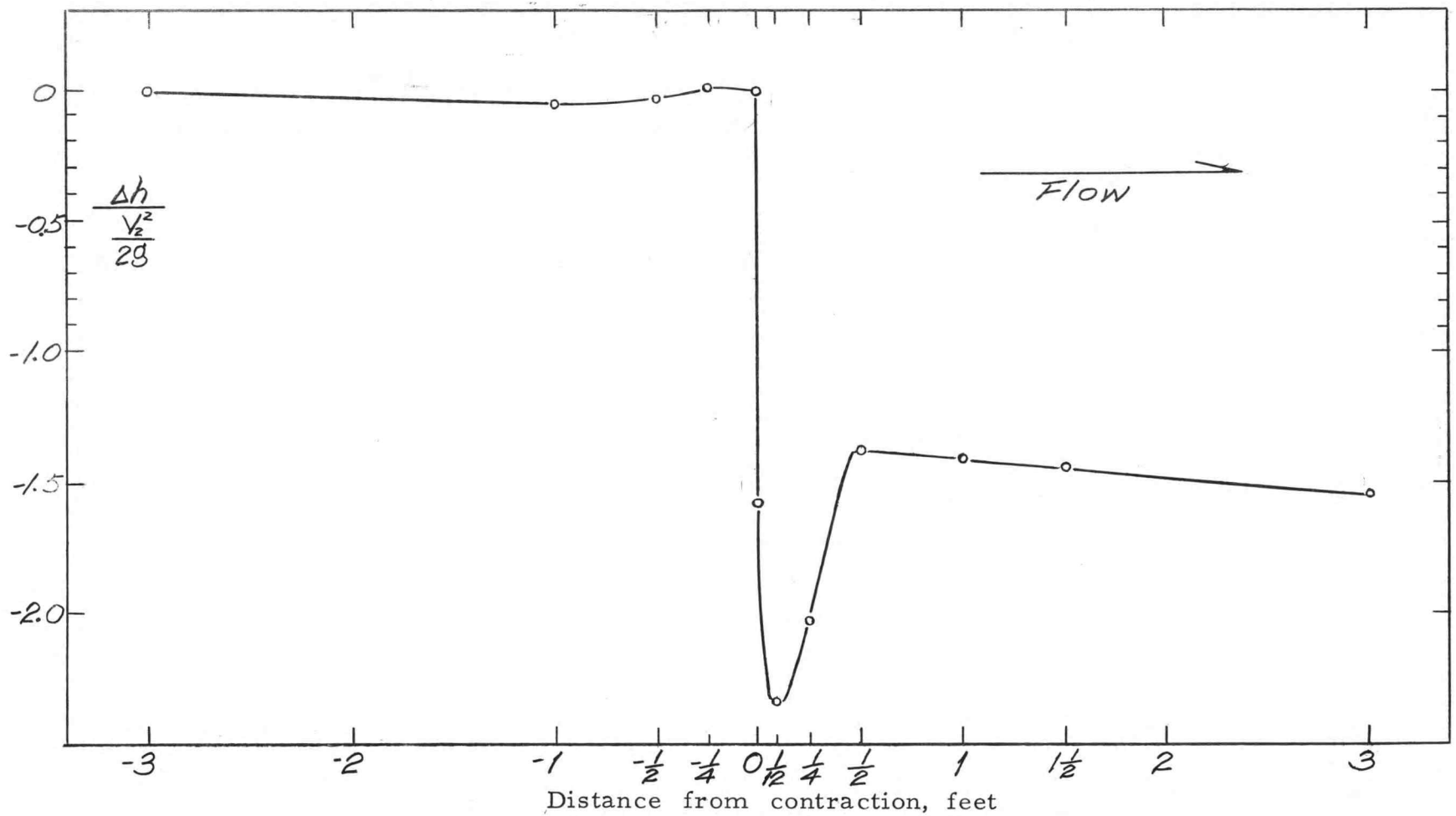

Figure 16 Peizometric head difference along boundaries

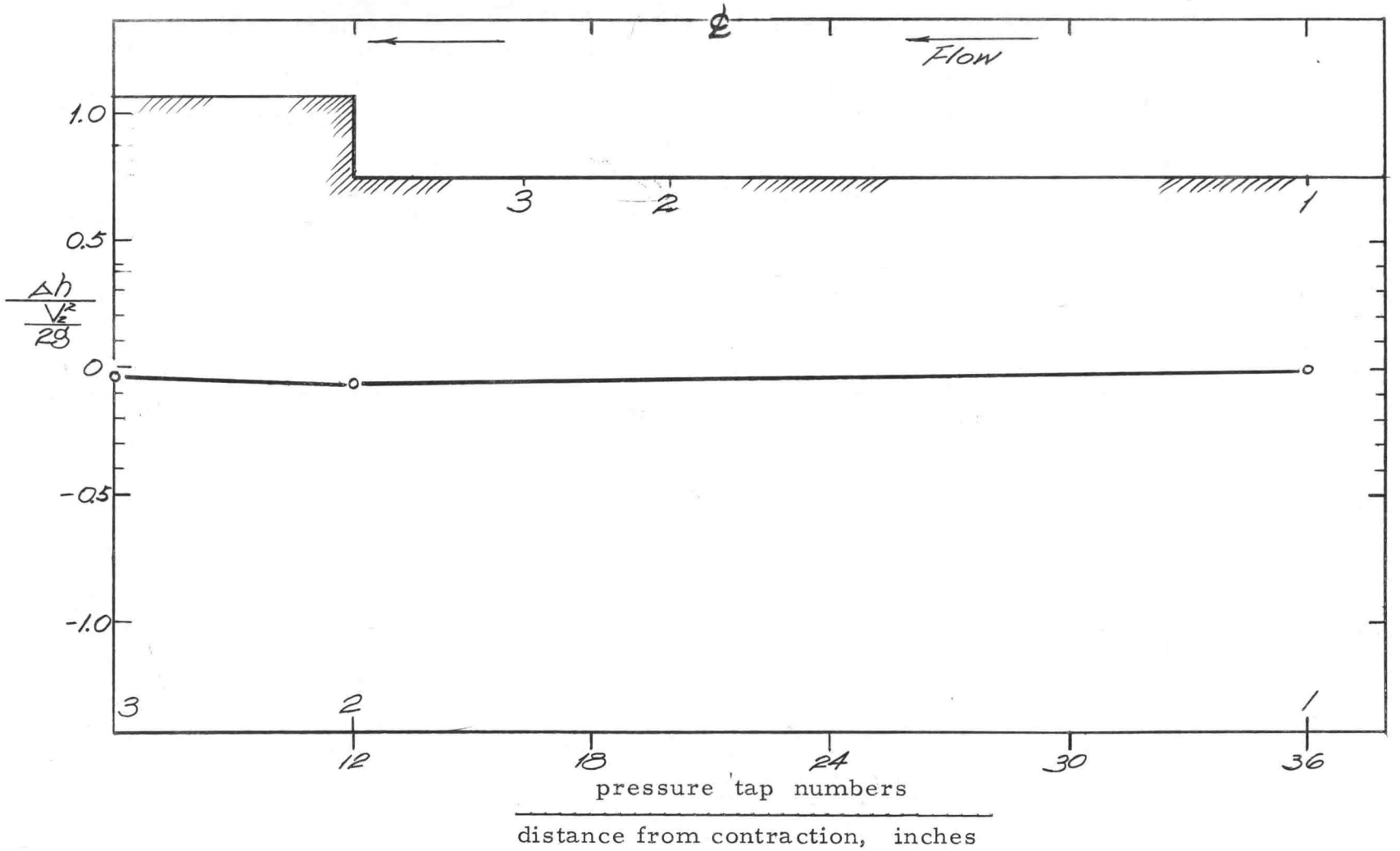

Figure 17 Piezometric head difference along upstream boundary

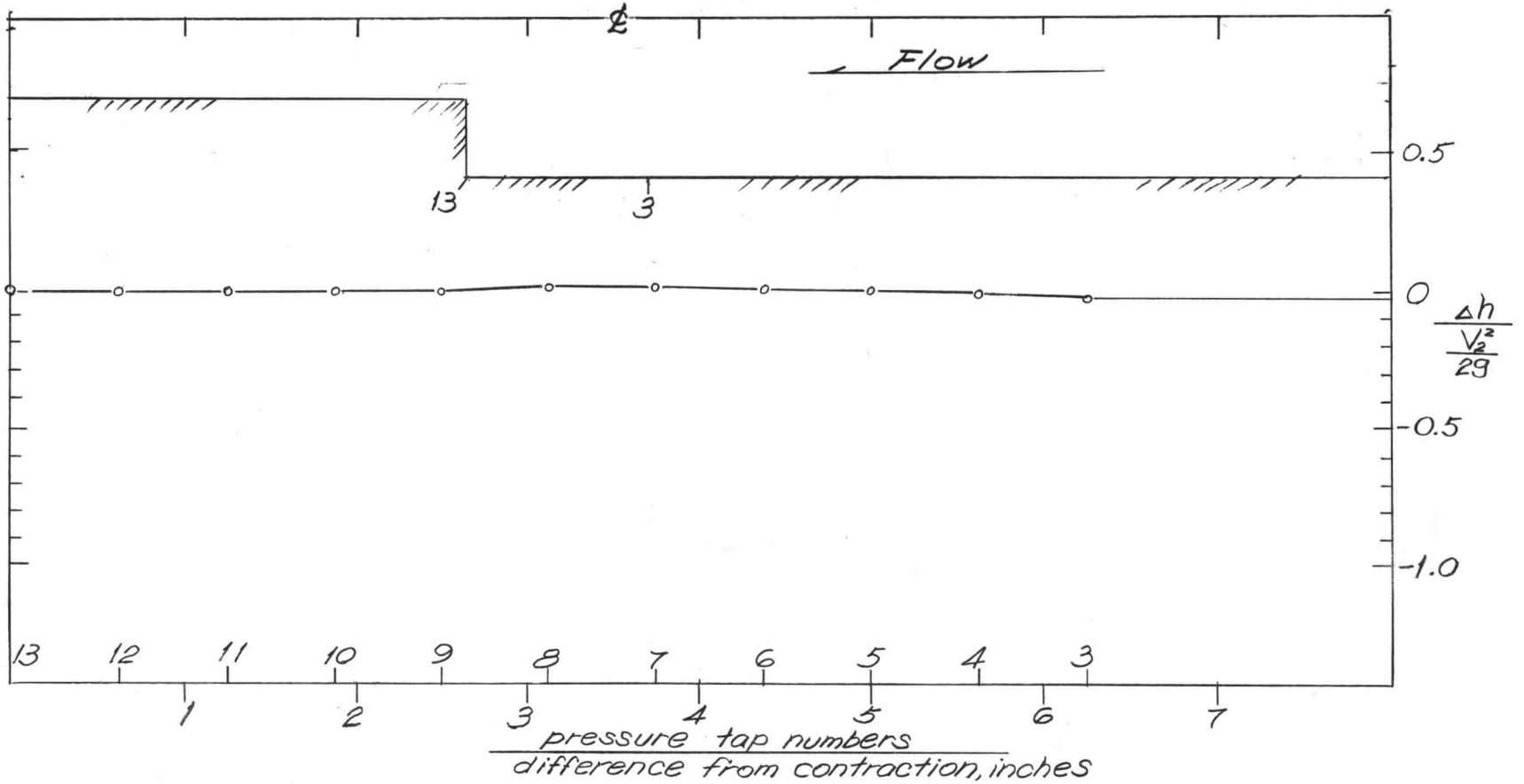

Figure 18. Piezometric head difference along upstream zone of discontinuity

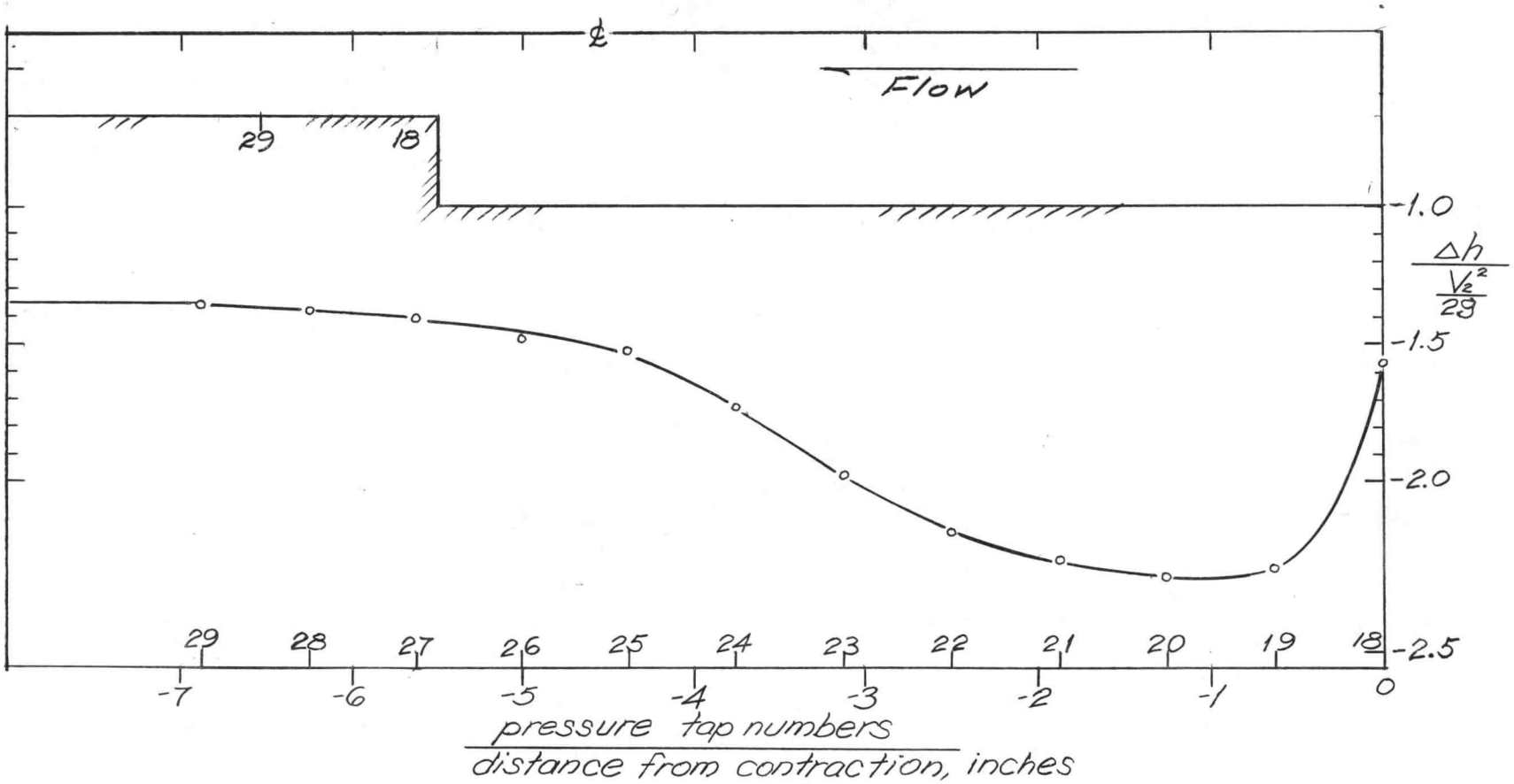

Figure 19. Piezometric head difference along boundary of downstream zone of discontinuity

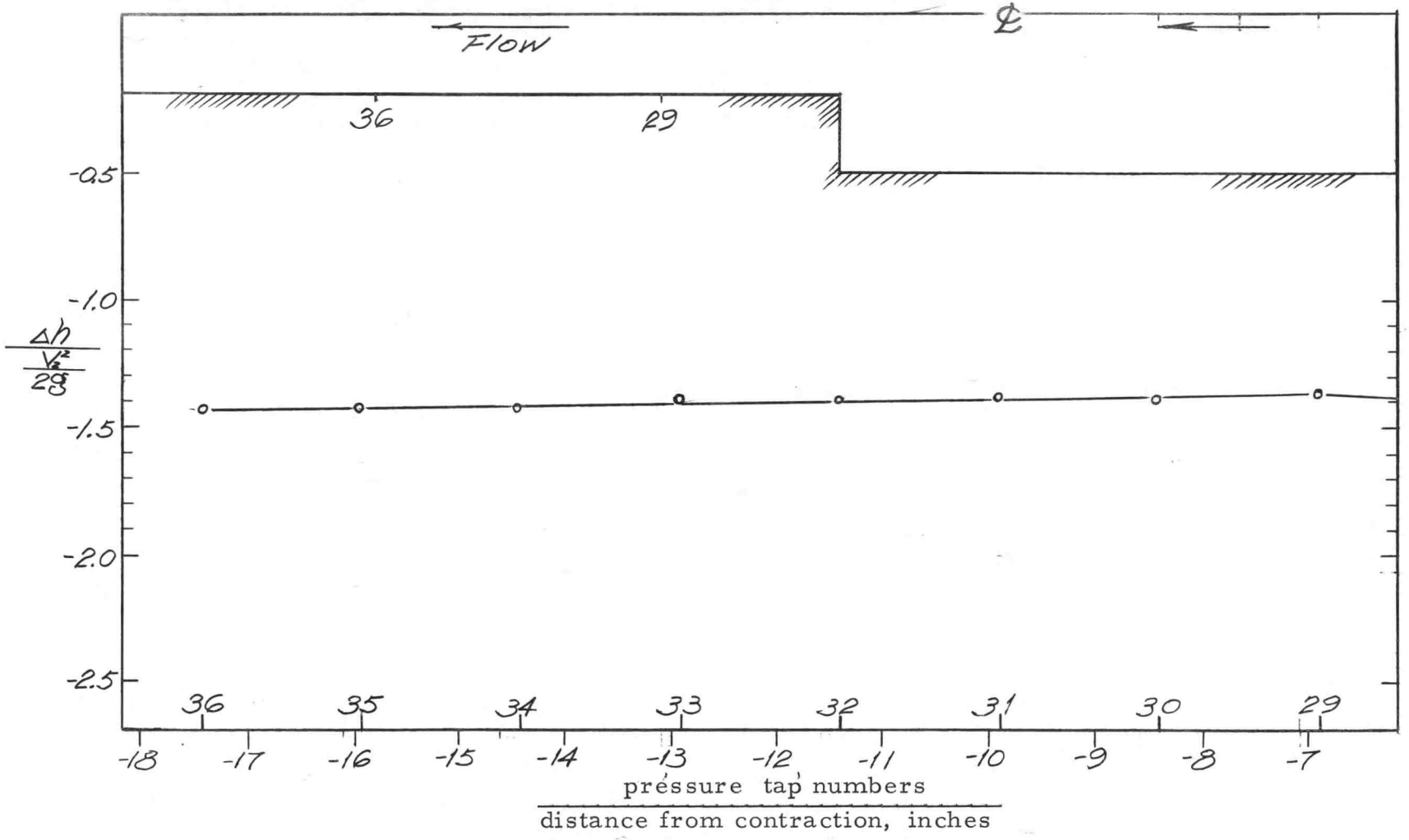

Figure 20 Piezometric head difference along downstream boundary

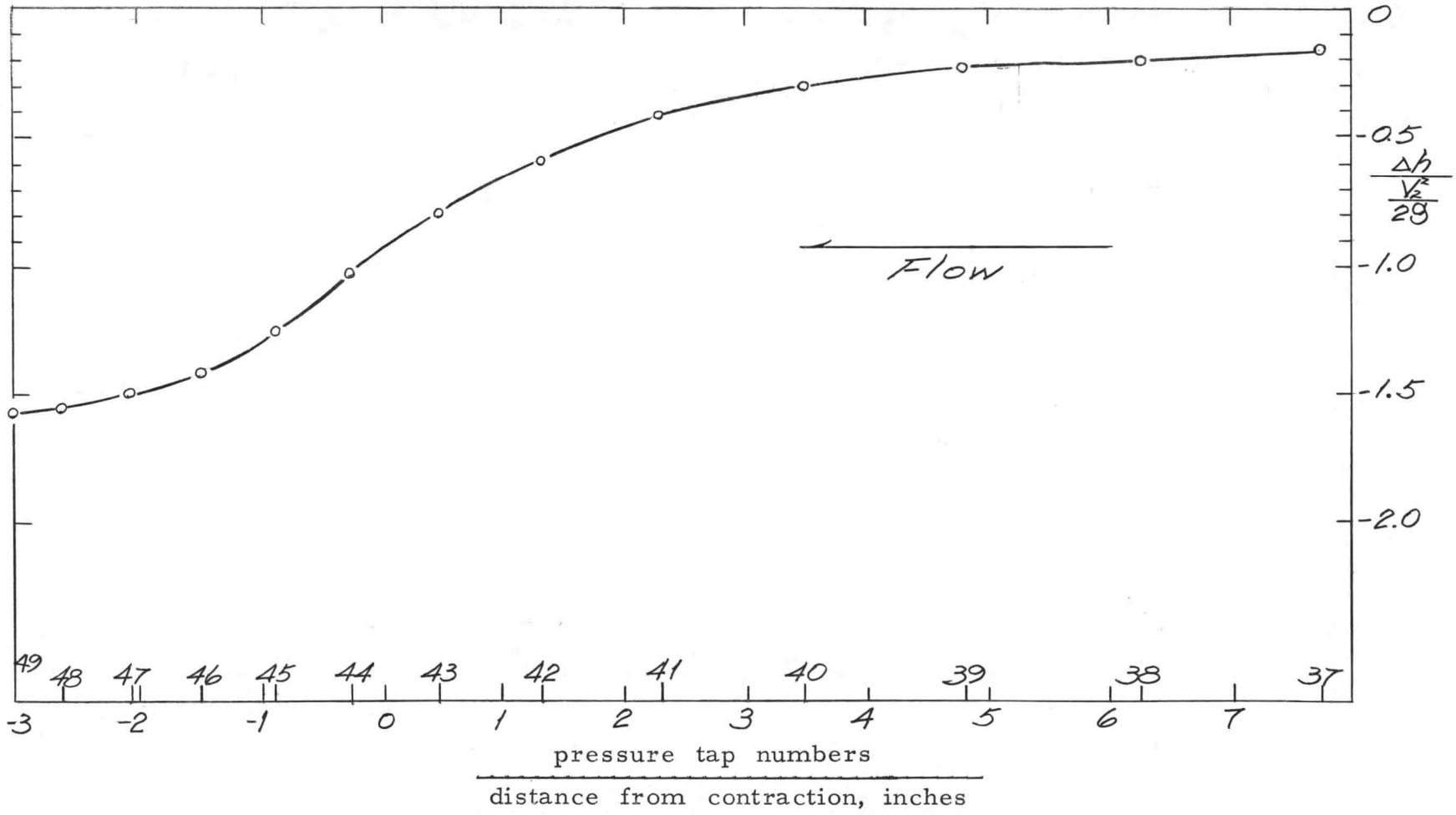

Figure 21 Piezometric head difference along center line in transition zone

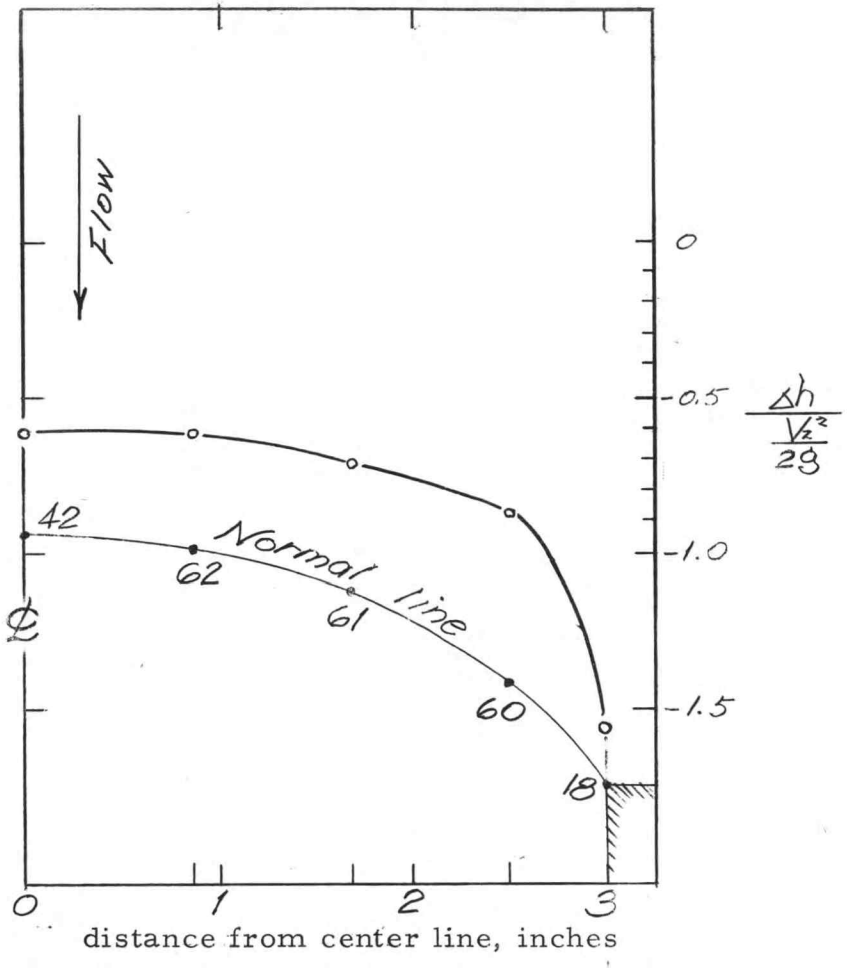

Figure 22 Piezometric head difference along normal line at the entrance of the smaller conduit

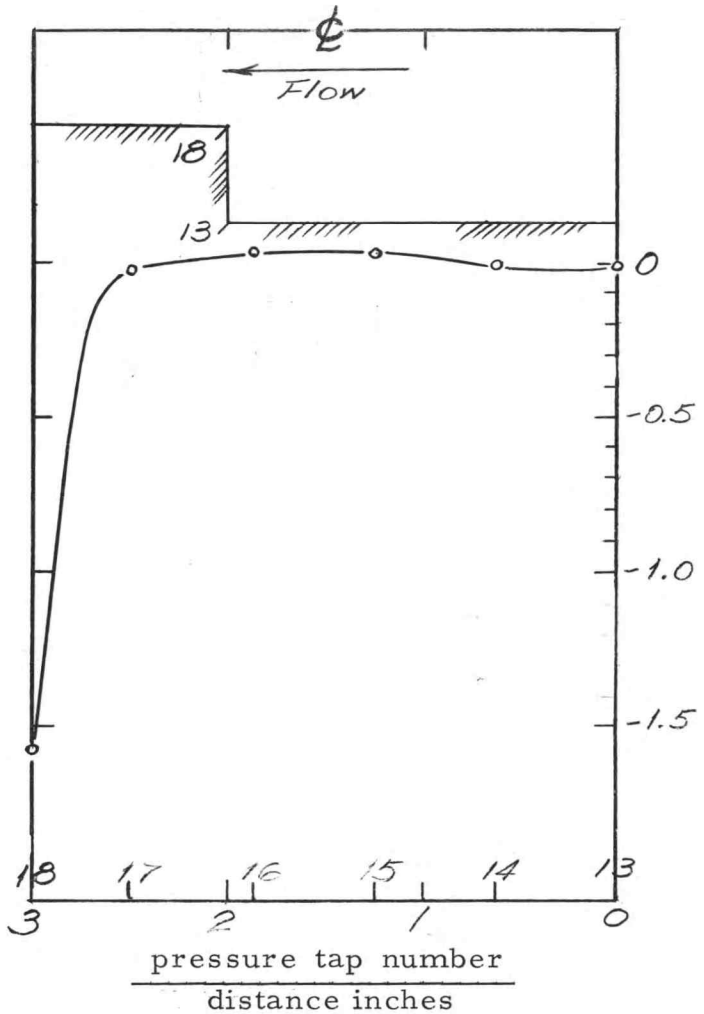

Figure 23 Piezometric head difference along vertical boundary

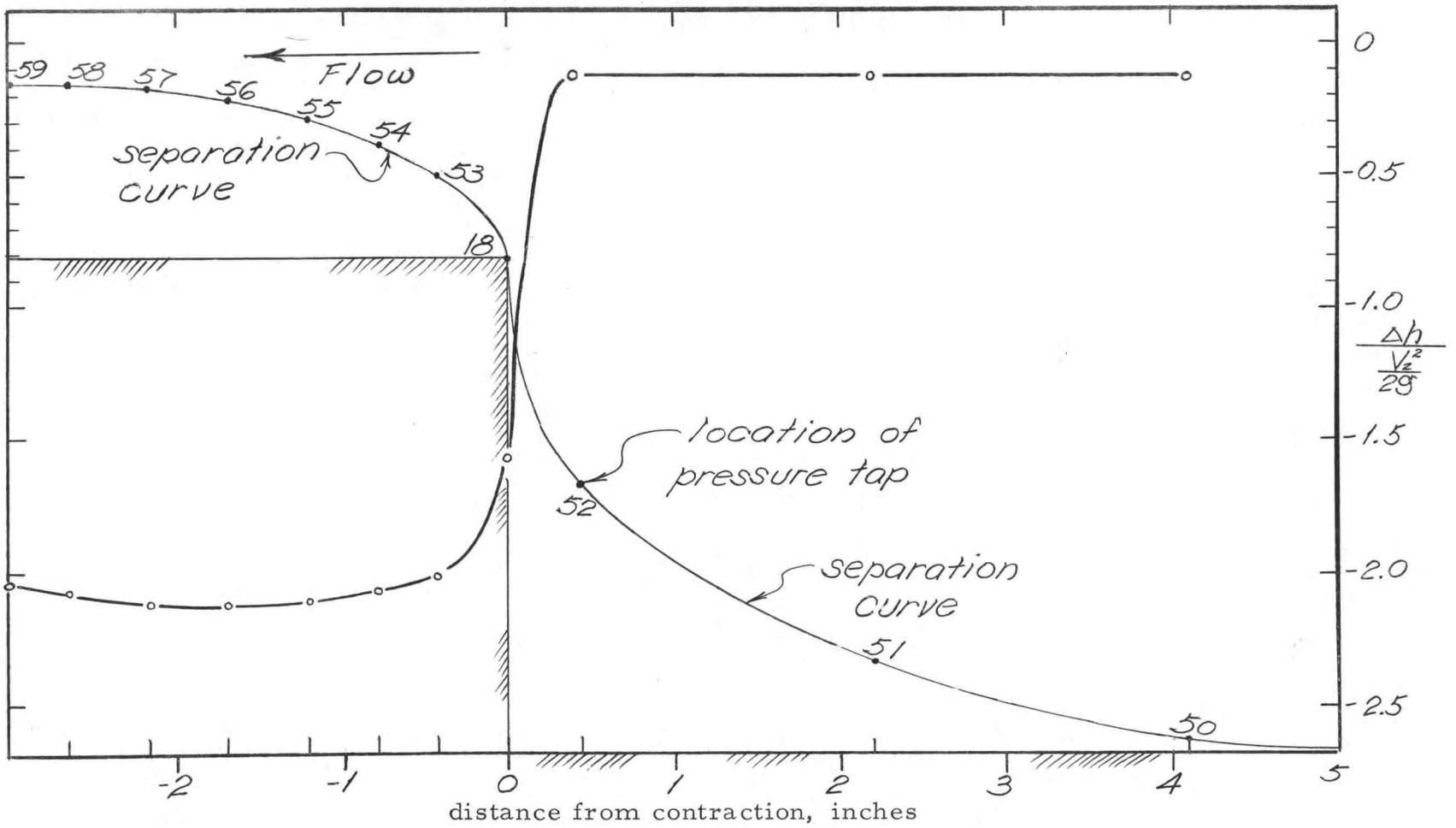

Figure 24 Piezometric head difference along separation curves

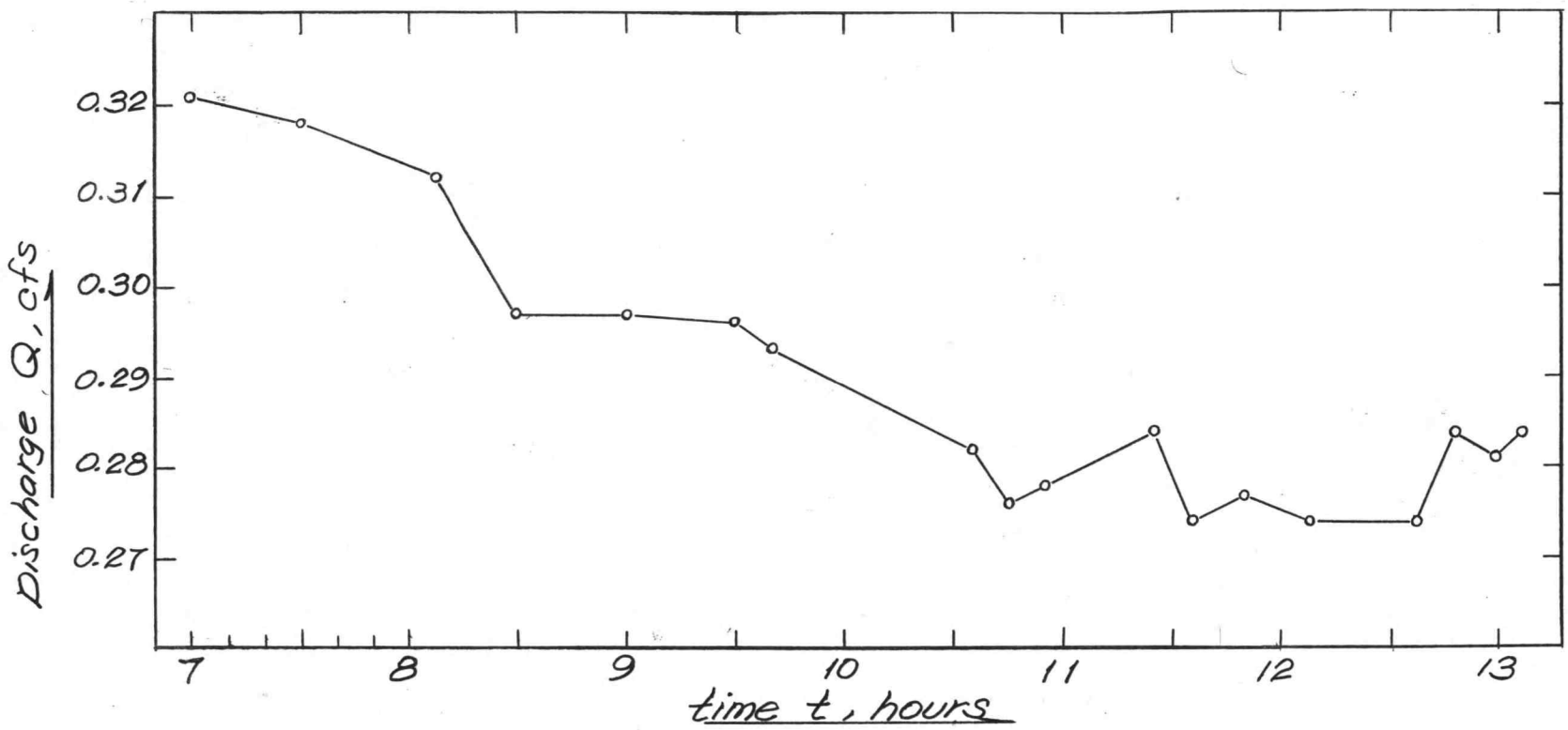

Figure 25 Variation of the rate of flow during the test

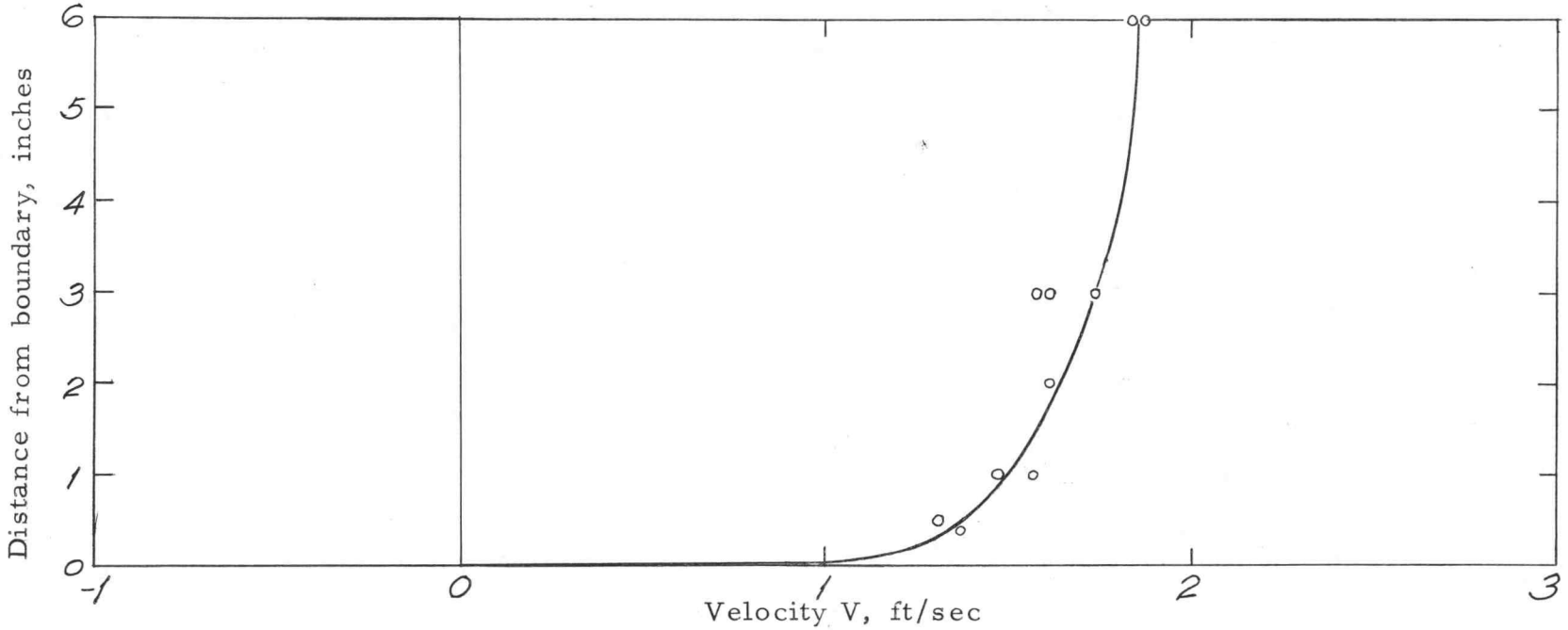

Figure 26 Velocity profile at section 1 ft. upstream from contraction

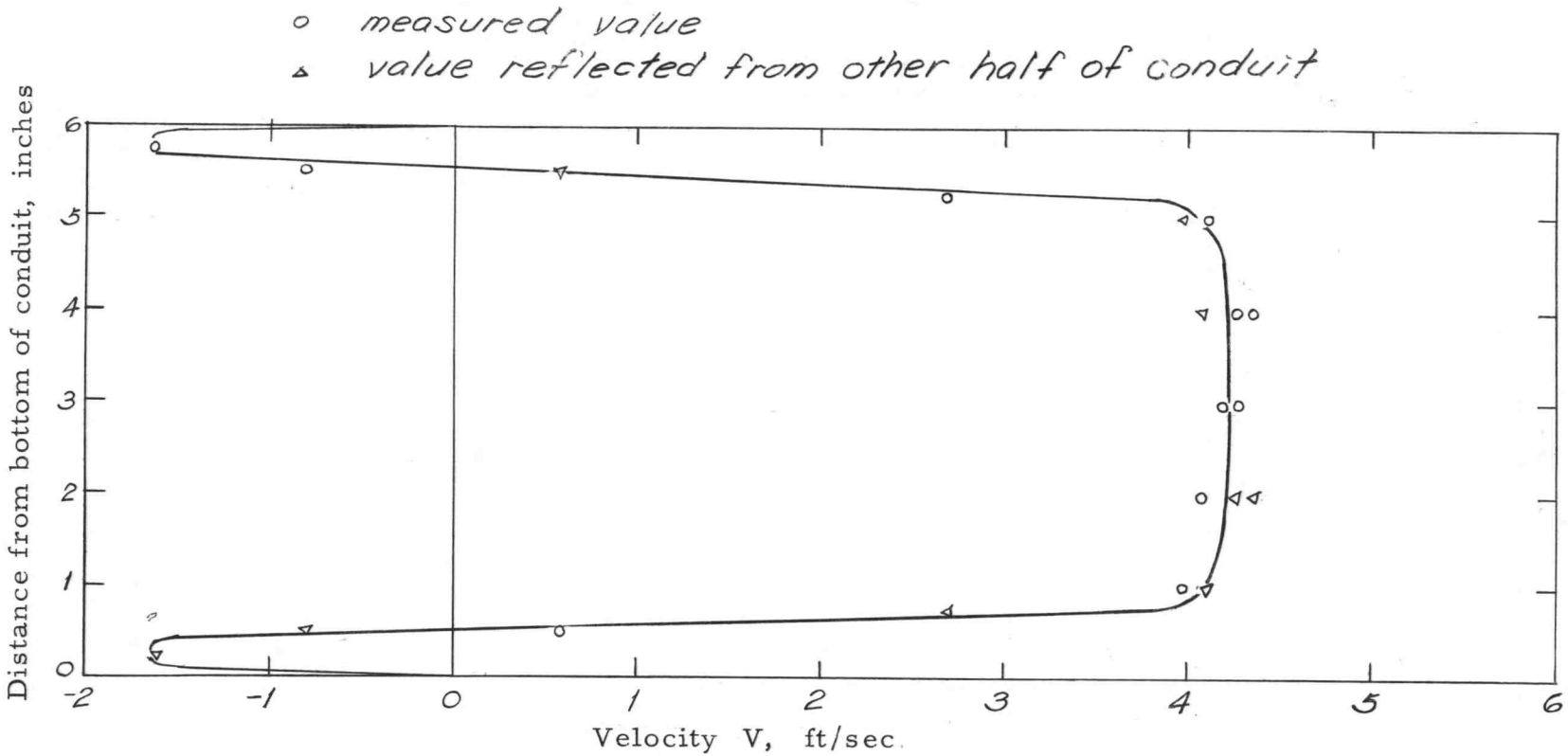

Figure 27 Velocity profile at section 3 inches downstream from contraction

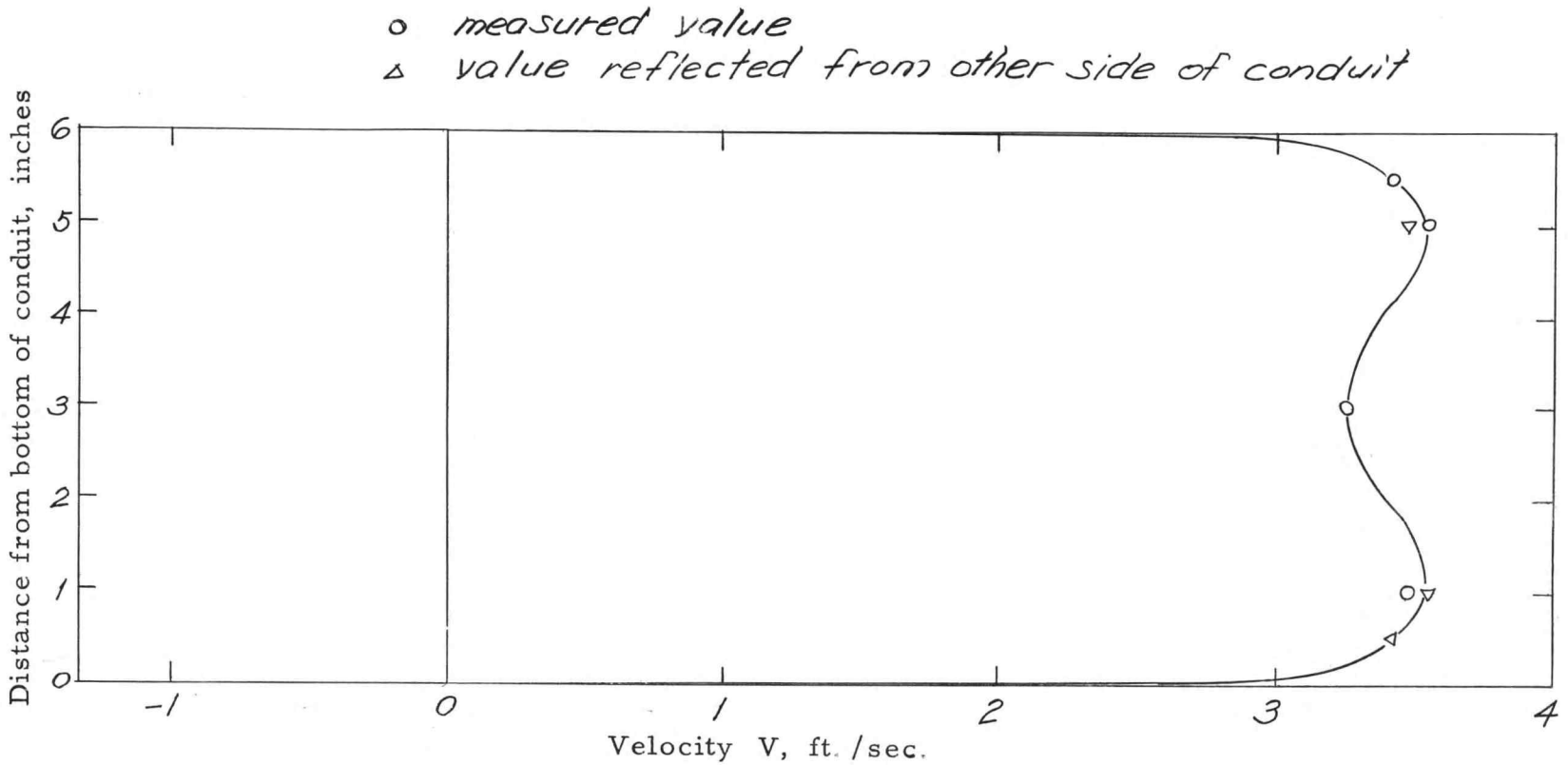

Figure 28. Velocity profile at section 3 feet downstream from contraction

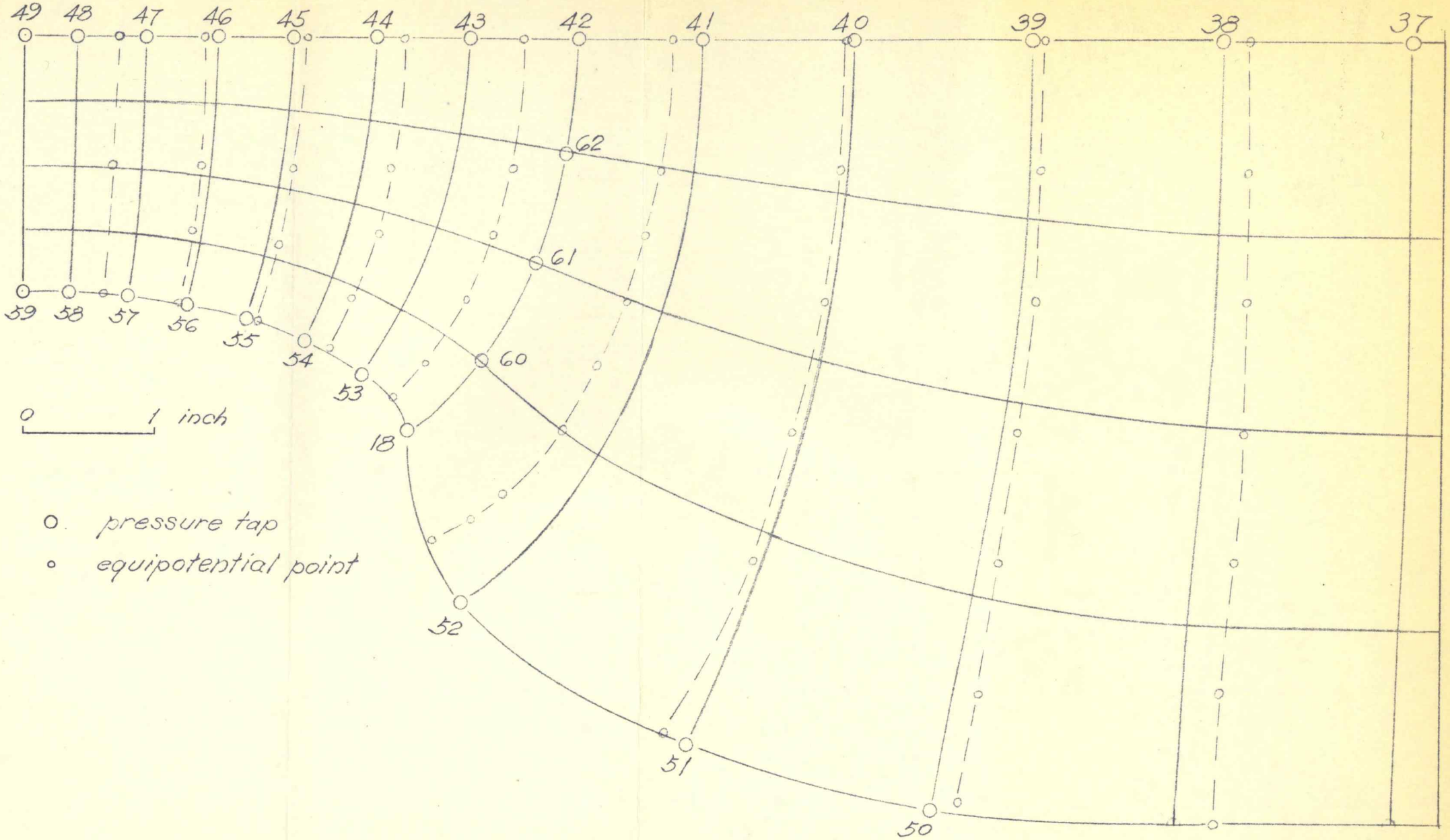

Figure 29. Measured equipotential lines, flow net and pressure connection locations

DISCUSSION

Separation curves

Separation curves were very difficult to determine from the photographs of the flow as may be seen in Figure 13 and Figure 14. Only approximate stream lines were drawn. Figure 15 shows the large deviation of curves obtained from different pictures. If the flow was symmetrical, the coefficient of contraction for the two dimensional contraction varied from 0.597 to 0.800.

The determined average downstream separation curve indicated a coefficient of contraction of 0.640 which is very close to the value of 0.644 obtained by von Mises. (6, p. 34).

To calculate the head loss along center line in transition zone, the ratio of velocity at point No.49 to point No. 37, V49/V37, was scaled from flow net and was equal to 3.125. The piezometric head difference actually measured between these points was 0.224 foot. Using the modification of Equation 6

$$\frac{\frac{H_L}{V_0^2}}{2g} = \frac{\frac{\Delta h}{V_0^2}}{2g} + \left[1 - \left(\frac{V}{V_0} \right)^2 \right] = -3.15$$

This negative result indicates that the velocity ratio scaled off the flow net was not correct, which in turn means that the determined separation curves could not represent the true surface of

discontinuity. Furthermore the surface of discontinuity in a two-dimensional conduit was observed to be warped along the central plane so that the average surface can not be determined merely by observation or photographing.

Irrotation Flow Pattern

From Figure 26 and Figure 27, it is apparent that the velocity distributions across approaching conduit and across the two-dimensional jet were quite uniform. This fact indicates that viscous shear was not appreciable in flow except in the relatively thin layers near the boundaries. Figure 22 shows the pressure along a normal line at the entrance to the smaller conduit. The variation of pressure in combination with velocity variation along this line also denotes a uniform distribution of energy in the acceleration zone. Thus the flow pattern may be considered irrotational as a close approximation.

Energy loss

The results of energy loss calculations show that in a two-dimensional conduit total loss caused by the boundary form change of sudden contraction with area ratio of 0.5 was $0.512 \frac{V_2^2}{2g}$, which is higher than the value $0.33 \frac{V_2^2}{2g}$ tabulated by Rouse (p. 265B).

Only 53.7 percent of the energy loss occurred downstream from the section near vena contracta. This value was calculated using average pressure across the section 3 inches downstream from contraction. Equation 15 will yield no reasonable head loss as may be seen from the computation of head losses presented in appendix.

Flow Observation and Pressure Gradient

From the results of the final observations of flow patterns, the piezometric pressure plots were found to give good interpretation of flow phenomena in the conduit. Careful observations of back flow in either upstream separation zone or downstream separation zone were made. The upstream separation curve was found to leave the boundary at a point about 3 inches upstream from the vertical wall, and to contact the vertical wall about 1 inch away from the square-edged entrance to the smaller conduit. Both points may be considered as points where velocity was zero, since the flow outside those points and the flow inside these points have contrary directions. From Figure 18 and Figure 23, the zero piezometric head gradients have clearly indicated the points where flow suddenly changed direction due to the existence of the separation curve.

The point where the downstream separation curve again contacted the boundary was observed to be located 4 or 5 inches downstream from the contraction. The only indication of the

existence of such point is the fact that most of the pressure has been regained and the positive pressure gradient that would cause backflow is decreasing thereafter.

The location of the vena contracta is apparent in Figure 24 where the pressure along separation curve starts to rise, indicating deceleration of the flow, hence the expansion of the jet. On this basis the vena contracta was found located at 2 1/4 inches downstream from contraction.

From Figure 24 the pressure along the assumed upstream separation curves was quite uniform. Energy dissipation along the upstream separation curve is indicated by the decrease of velocity in combination with the uniform distribution of pressure. Since the velocity of the surrounding flow is very low, only a small amount of head loss is expected to be dissipated in the upstream zone of discontinuity. A small negative pressure gradient may be seen existing along the downstream separation curve. If the velocity along surface of discontinuity is constant as in a free jet, the decreasing pressure gives a good estimation of the energy dissipation along the surface of discontinuity.

A constant negative boundary pressure gradient begins at 6 7/8 inches downstream from contraction. From this finding it may be interpreted that downstream from this point energy loss is not affected by the sudden contraction.

Pressure Across Section Near Vena Contracta

As mentioned before, velocity distribution was rather uniform in the confined jet at the section 3 inch downstream from contraction, and the flow pattern in jet could be considered irrotational, thus the pressure across the cross-section was expected to be uniformly distributed in jet. However, the contrary was found to be the case, as may be seen from Figure 29. The pressure at separation curve was smaller than that at center line. This pressure difference may be considered to be caused by a normal acceleration.

CONCLUSIONS

The foregoing discussions lead to the following conclusions.

1. Energy distribution and dissipation in a transition region of a two-dimensional sudden contraction can not be computed because correct separation curves can not be determined and the flow net therefrom constructed yields only approximate distribution of velocities.

2. The loss coefficient of a two-dimensional conduit sudden contraction is found equal to 0.512.

3. Determination of flow separation curves in a two-dimensional conduit by observation and photographing does not yield satisfactory results to study irrotational flow pattern.

4. The coefficient of contraction is 0.792 for a square-edged sudden contraction of two-dimensional geometry. The location of the vena contracta is at the section 2 1/4 inches downstream from the contraction.

5. The pressure across the assumed vena contracta is not uniform. The variation of pressure is caused by the existence of normal acceleration.

6. The upstream separation curve begins at the point 3 inches (1/2 smaller conduit height) upstream of the contraction and stops on the vertical wall at 1 inch away from the square-edged entrance of the smaller conduit. The downstream separation begins at the

downstream corner and closes the downstream zone of continuity at the point 5 inches from the contraction.

7. Flow domain bounded by either boundaries or separation curves may be considered as irrotational flow pattern.

RECOMMENDATIONS

1. The energy distribution in the transition zone of a two-dimensional sudden contraction can be determined by measuring total head at different points in this zone using measuring devices of high sensitivity.

2. It would be of interest to study the flow pattern and its energy dissipation in the mixing zone.

3. More information is needed about the characteristics of confined jets.

4. The model arrangement in this experiment is recommended for further study on two-dimensional flow problems, except that the conduit should be installed horizontally with side walls parallel to floor and that a larger stilling tank and more sensitive valve should be used to obtain constant head water surface. It is also recommended that the upstream No. 18 wire screen be taken off to assure a steady flow.

BIBLIOGRAPHY

1. Curtis D. D. et al. Coefficient of contraction for a submerged jet. A.S.C.E. Hydraulic Journal 82: 1038-17, 1038-20. 1956.

2. Dodge R. A. Fluid mechanics. New York, McGraw-Hill, 1937. 495 p.

3. Heacock H. W. An experimental determination of coefficients for the contraction and diffusion of submerged jets in series. Master's thesis. Corvallis, Oregon State University, 1958. 75 numbered leaves.

4. King H. W. et al. Hydraulics. New York, Wiley, 1941. 303 p.

5. Krynine D. P. Soil mechanics. New York, McGraw-Hill, 1947. 511 p.

6. Rouse, Hunter. Elementry mechanics of fluids. New York, Wiley, 1946. 376 p.

7. Rouse, Hunter. Engineering hydraulics. Proceedings of the fourth hydraulics conference, Iowa institute of hydraulics research. New York, Wiley, 1950. 1039 p.

8. Rouse, Hunter. Fluid mechanics for hydraulic engineers. New York, McGraw-Hill, 1938. 422 p.

9. Streeter, Y. L. Fluid mechanics. New York, McGraw-Hill. 1958. 480 p.

10. Vennard J. K. Elementary fluid mechanics. New York, Wiley, 1954. 401 p.

11. Worth J. E. Establishment of velocity profiles in a liquid downstream from a sudden pipe contraction. Master's thesis. Corvallis, Oregon State University, 1961. 77 numbered leaves.

APPENDIX

Determination of specific gravity of chloroform

	Left column inches	Right column inches
Water surface	11.47	15.48
Chloroform surface	4.39	- 4.15
Difference in length of H_2O column	7.08	19.63

$$19.63 - 7.08 = S_c(4.39 + 4.15)$$

$$S_c = 1.47 \qquad \Delta S = S_c - S_w = 0.47$$

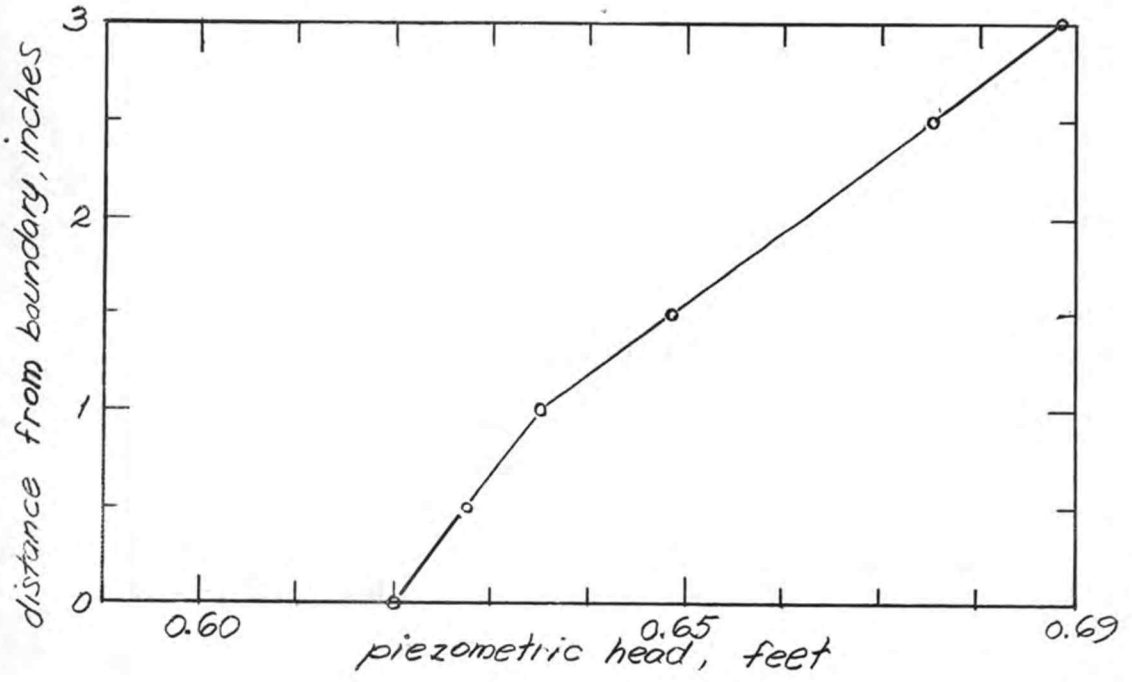

Figure 30. Head across section 3 inches downstream from contraction.

Velocity Corrections

Table 10

Velocity profile at section 1 foot upstream from contraction

Distance from top H inch	Manometer reading Δh inch	Velocity V ft./sec.	Correction factor $\frac{Q}{Q_0}$	Corrected velocity V_c ft./sec.
3	0.96	1.55	1.01	1.57 +
6	1.23	1.76	1.04	1.83
3	0.91	1.51	1.07	1.62 +
1	0.74	1.36	1.08	1.47
$\frac{1}{2}$	0.68	1.21	1.08	1.31
0.4	0.64	1.27	1.08	1.37
9	1.50	1.94	1.08	2.10 *
6	1.18	1.72	1.085	1.87
3	1.00	1.59	1.085	1.73
2	0.84	1.46	1.10	1.61
1.5	0.82	1.43	1.105	1.58
1	0.80	1.42	1.105	1.57

Q_0 = 0.321 c.f.s.
* high, due to vibration of pitot tube tip.
+ low.

Table 11

Velocity profile at section 3 inches downstream from contraction

Distance from top H inch	Manometer reading Δh inch	Velocity V ft./sec.	Correction factor $\frac{Q}{Q_0}$	Corrected velocity V_c ft./sec.
3	5.68	3.78	1.13	4.27
4	5.84	3.83	1.13	4.35
3	5.36	3.68	1.14	4.19
4	5.36	3.68	1.16	4.26
5	4.98	3.53	1.16	4.10
$5\frac{1}{2}$	- 0.20	- 0.71	1.15	- 0.82
$5\frac{1}{4}$	2.22	2.36	1.14	2.69
$5\frac{3}{4}$	- 0.82	- 1.43	1.14	- 1.63
2	4.80	3.48	1.17	4.07
1	4.67	3.43	1.16	3.98
$\frac{1}{2}$	0.10	0.50	1.17	0.59

Q_0 = 0.321 c.f.s.

Table 12

Velocity profile at section 3 feet downstream from contraction

Distance from top H inch	Manometer reading Δh inch	Velocity V ft./sec.	Correction factor $\frac{Q}{Q_0}$	Corrected velocity V_c ft./sec.
3	3.15	2.82	1.150	3.25
5	3.72	3.06	1.135	3.48
3	3.30	2.88	1.138	3.27
$5\frac{1}{2}$	3.56	3.00	1.135	3.41
1	3.89	3.13	1.130	3.54

Q_0 = 0.321 c.f.s.

Velocity Coefficients

Table 13

Velocity coefficients at section 1 foot upstream from contraction

Distance from boundary H inches	Velocity v ft./sec.	$\left(\frac{v}{V}\right)$	$\left(\frac{v}{V}\right)^2$	$\left(\frac{v}{V}\right)^3$
$\frac{1}{2}$	1.35	0.804	0.647	0.520
$1\frac{1}{2}$	1.58	0.941	0.885	0.832
$2\frac{1}{2}$	1.71	1.018	1.034	1.052
$3\frac{1}{2}$	1.79	1.066	1.135	1.210
$4\frac{1}{2}$	1.82	1.083	1.174	1.270
$5\frac{1}{2}$	1.83	1.089	1.183	1.288
	10.08		6.058	6.172
	1.68 = V		1.010 = Km	1.029 = Ke

$\frac{1.68}{1.605} = 1.05$

5% error is due to three-dimensional effect.

Table 14

Velocity coefficients at section 3 inches downstream from contraction

Distance from boundary H inch	Velocity v ft./sec.	$\left(\frac{v}{V}\right)$	$\left(\frac{v}{V}\right)^2$	$\left(\frac{v}{V}\right)^3$
$1\frac{1}{4}$	4.17	0.984	0.969	0.953
$1\frac{3}{4}$	4.28	1.010	1.020	1.032
$2\frac{1}{4}$	4.27	1.008	1.012	1.020
$2\frac{3}{4}$	4.23	0.998	0.995	0.993
Σ	16.95		3.996	3.998
	4.24		0.999	0.999
	= Average jet velocity		$\doteq$ 1.000	$\doteq$ 1.000
$Cc = \frac{2 \times 1.68}{4.24} = 0.792$			= Km	= Ke

Table 15

Velocity coefficients at section 3 feet downstream from contraction

Distance from boundary H inches	Velocity v ft./sec.	$\left(\frac{v}{V}\right)$	$\left(\frac{v}{V}\right)^2$	$\left(\frac{v}{V}\right)^3$
$\frac{1}{4}$	3.25	0.958	0.918	0.879
$\frac{3}{4}$	3.51	1.034	1.070	1.106
$1\frac{1}{4}$	3.53	1.040	1.081	1.125
$1\frac{3}{4}$	3.43	1.010	1.020	1.030
$2\frac{1}{4}$	3.35	0.988	0.976	0.965
$2\frac{3}{4}$	3.29	0.970	0.940	0.912
Σ	20.36		6.005	6.017
	3.393		1.001	1.003
	= V		= Km	= Ke

$$\frac{V}{V_t} = \frac{3.393}{3.210} = 1.058$$

5% error due to three dimensional velocity distribution.

Energy Loss Calculations

Energy loss between section 1 foot upstream and section 3 feet downstream from contraction

From Table 13 and Table 15

$V_{d.s.} = 3.21$ ft./sec. $\quad Ke = 1.003$

$V_{u.s.} = 1.605$ ft./sec. $\quad Ke = 1.029$

From Figure 16 and Table 6

$\Delta h = -0.930 + 0.682 = 0.248$ ft.

Entering Equation 10.

$$E_{L_{1-3}} = \Delta h + \frac{v_1^2}{2g} Ke_2 - \frac{v_2^2}{2g} Ke_1$$

$$= 0.248 + \frac{(3.21)^2 (1.003) - (1.605)^2 (1.029)}{64.4}$$

$$= 0.128 \text{ ft.}$$

Energy loss between section 3 inches downstream from contraction and section 3 feet downstream from contraction

From Table 14 and Table 15

$V_1 = 4.24$ ft./sec. $\quad V_2 = 3.21$ ft./sec.

$Ke_1 = 1.000 \quad Ke_2 = 1.003$

$Km_1 = 1.000 \quad Km_2 = 1.001$

Entering Equation 15

$$E_{L_{2-3}} = \frac{1}{2g} \left[(2 Km_2 - Ke_2) V_2^2 - 2Km_1 V_1 V_2 + Ke_1 V_1^2 \right]$$

$$= \frac{1}{64.4} \left[(2(1.001) - 1.003)(3.21)^2 - 2(1.000)(3.21)(4.24) + 1.000(4.24)^2 \right]$$

$$E_{L_{2-3}} = 0.013 \text{ ft.}$$

This head loss was also computed using one-dimensional energy equation.

Pressure across the section 3 inches downstream from contraction was not uniform. From Figure 30 value of average pressure was computed.

$$P_1 = \frac{1}{3}(0.675 + 0.649 + 0.627)$$

$$= 0.650$$

From Table 6

$$P_2 = 0.682 \qquad \Delta h = -0.032$$

Entering Equation 10

$$E_{L_{2-3}} = \Delta h - \frac{Ke_2 V_2^2}{2g} - Ke_1 \frac{V_1^2}{2g}$$

$$= 0.032 - \frac{(3.21)^2}{64.4}(1.003) - \frac{(4.24)^2}{64.4}(1.00)$$

$$= 0.032 + 0.118$$

$$= 0.086 \text{ ft.}$$

Energy loss due to pipe friction

Assuming constant friction factor, equation 13 is used to calculate friction loss.

From Figure 6, the coefficient K was measured equal to 0.004 for upstream conduit and 0.014 for smaller conduit. Therefore, the loss between upstream section and contraction is

$$E_{L_U} = KL = 0.004 \times 1 = 0.004 \text{ ft.}$$

and the loss between contraction and downstream section is

$$E_{L_D} = 0.014 \times 3 = 0.042 \text{ ft.}$$

Total head loss due to boundary change is

$$E'_{L_{1-3}} = E_{L_{1-3}} - (E_{L_U} + E_{L_D}) = 0.082 \text{ ft.}$$

$$= 0.512 \frac{V_2^2}{2g}$$

and head loss due to jet expansion is

$$E'_{L_{2-3}} = E_{L_{2-3}} - E_{L_D} = 0.044 \text{ ft.}$$

$$= 0.275 \frac{V_2^2}{2g}$$

where $E_{L_{2-3}}$ is the value obtained by using Equation 10.

About 54 percent total loss due to boundary form change occurred in mixing zone. This finding for a conduit of two-dimensional geometry is not far from the result obtained by Worth for a three dimensional pipe sudden contraction.

The value, 0.013 ft., computed from Equation 15 is too small to be considered as a reasonable head loss. Since $E_{L_{2-3}}$ can not be smaller than E_{LD}.

This different result is possibly caused by the fact that the assumption of negligible shear along boundaries is not true.